Article

Cell Host & Microbe

Deep tissue infection by an invasive human fungal pathogen requires lipid-based suppression of the IL-17 response

Graphical abstract

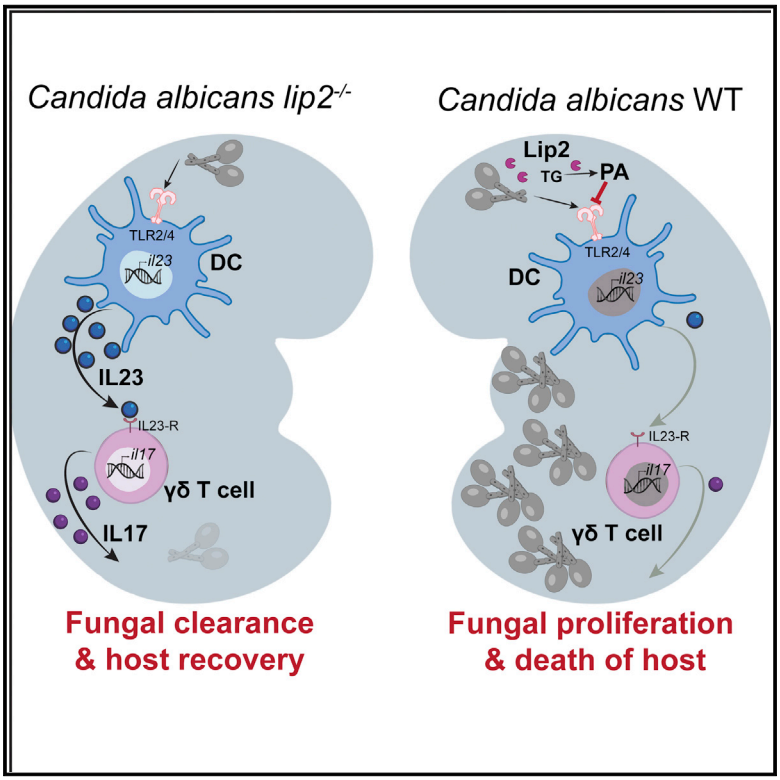

Authors

Pauline Basso, Eric V. Dang, Anatoly Urisman, Leah E. Cowen, Hiten D. Madhani, Suzanne M. Noble

Correspondence

pauline.basso@ucsf.edu (P.B.), suzanne.noble@ucsf.edu (S.M.N.)

In brief

In a murine model of systemic fungal infection, Basso et al. show that *C. albicans* secreted lipase, Lip2, suppresses local antifungal IL-17 responses in infected organs by altering dendritic cell activation. Under *in vitro* conditions, the immunosuppressive activity of Lip2 is mimicked by palmitic acid, a product of Lip2 hydrolysis.

Highlights

- The secreted lipase Lip2 is required for *C. albicans* virulence in the bloodstream
- Lip2 suppresses an antifungal IL-17 response in infected internal organs
- Lip2 indirectly impacts IL-17 by suppressing IL-23 production by dendritic cells
- Lipase product palmitic acid mimics the activity of Lip2 on cultured dendritic cells

Basso et al., 2022, Cell Host & Microbe *30*, 1589–1601
November 9, 2022
https://doi.org/10.1016/j.chom.2022.10.004

CellPress

Cell Host & Microbe

CellPress
OPEN ACCESS

Article

Deep tissue infection by an invasive human fungal pathogen requires lipid-based suppression of the IL-17 response

Pauline Basso,[1,*] Eric V. Dang,[3] Anatoly Urisman,[4] Leah E. Cowen,[5] Hiten D. Madhani,[3] and Suzanne M. Noble[1,2,6,*]
[1]Department of Microbiology and Immunology, University of California San Francisco, San Francisco, CA 94143, USA
[2]Division of Infectious Diseases, Department of Medicine, University of California San Francisco, San Francisco, CA 94143, USA
[3]Department of Biochemistry and Biophysics, University of California San Francisco, San Francisco, CA 94158, USA
[4]Department of Pathology, University of California San Francisco, San Francisco, CA 94143, USA
[5]Department of Molecular Genetics, University of Toronto, Toronto, ON M5G 1M1, Canada
[6]Lead contact
*Correspondence: pauline.basso@ucsf.edu (P.B.), suzanne.noble@ucsf.edu (S.M.N.)
https://doi.org/10.1016/j.chom.2022.10.004

SUMMARY

Candida albicans is the most common cause of fungal infection in humans. IL-17 is critical for defense against superficial fungal infections, but the role of this response in invasive disease is less understood. We show that *C. albicans* secretes a lipase, Lip2, that facilitates invasive disease via lipid-based suppression of the IL-17 response. Lip2 was identified as an essential virulence factor in a forward genetic screen in a mouse model of bloodstream infection. Murine infection with *C. albicans* strains lacking Lip2 display exaggerated IL-17 responses that lead to fungal clearance from solid organs and host survival. Both IL-17 signaling and lipase activity are required for Lip2-mediated suppression. Lip2 inhibits IL-17 production indirectly by suppressing IL-23 production by tissue-resident dendritic cells. The lipase hydrolysis product, palmitic acid, similarly suppresses dendritic cell activation *in vitro*. Thus, *C. albicans* suppresses antifungal IL-17 defense in solid organs by altering the tissue lipid milieu.

INTRODUCTION

Fungal pathogens kill roughly 1.5 million people every year (Brown et al., 2012). Despite the enormous burden of fungal infectious disease, our understanding of pathogenic fungi lags well behind that of viruses, bacteria, and parasites of similar clinical importance, and we are only beginning to define rules governing interactions between fungi and mammalian hosts. This knowledge gap has contributed to a dearth of tools for timely diagnosis and treatment of fungal infections, and no vaccines are available for the prevention of any fungal disease (Brown et al., 2012).

Unusually for a fungus, the yeast *Candida albicans* is a stable component of mammalian gut, skin, and genitourinary microbiota (Hallen-Adams and Suh, 2017). Commensal colonization is asymptomatic, and recent studies suggest that gut colonization confers immune benefits to the host (Bacher et al., 2019; Jiang et al., 2017). In contrast, fungal overgrowth or escape into ectopic niches can produce a spectrum of noxious symptoms (Pfaller et al., 2006). The most common syndrome of "mucocutaneous candidiasis" comprises relatively superficial infections of the mouth, skin, nails, and female reproductive tract. Superficial candidiasis occurs in hosts of any age or immune status, and there are hundreds of millions of such cases every year, across the globe (Denning et al., 2018). By contrast, "systemic candidiasis" describes rarer, invasive infections that involve the bloodstream and internal organs. Unlike mucocutaneous disease, systemic infections occur most often in patients with underlying risk factors, such as immunodeficiency (either spontaneous or drug-induced), epithelial damage (such as following surgery and other invasive procedures), and microbial dysbiosis (typically following treatment with antibiotics) (Pfaller and Diekema, 2007). In keeping with the high concentration of these risk factors among hospitalized patients, *Candida* species are currently the fourth most common cause of bloodstream infection in US hospitals (Edmond et al., 1999), and mortality from systemic disease remains high at ~40% (Pfaller et al., 2012).

Insights into host defenses against candidiasis have emerged from studies of families with inherited predispositions to such infections. For example, the critical role played by IL-17 signaling in defense against superficial fungal infections emerged from studies of families with chronic mucocutaneous candidiasis (CMC), a syndrome of persistent or recurrent *C. albicans* infections of the mouth, skin, nails, and/or vulvovaginal tract (Huppler et al., 2012). CMC has been linked to independent mutations affecting IL-17F (Puel et al., 2011), a component of IL-17 cytokines, as well as IL-17RA and IL-17RC (Lévy et al., 2016; Ling

et al., 2015; Puel et al., 2011), which together compose the heterodimeric IL-17 receptor. IL-17 signaling molecules are highly conserved, and null alleles affecting mouse orthologs also confer enhanced susceptibility to superficial *C. albicans* infections (Conti et al., 2009). Interestingly, however, humans with isolated CMC or treated with inhibitors of IL-17 signaling are not at higher risk for *C. albicans* bloodstream infections (Sparber and LeibundGut-Landmann, 2019), reinforcing the perception that IL-17 plays a less significant role in controlling systemic fungal disease.

In this study, we identify a *C. albicans* secreted lipase, Lip2, that is required for virulence in a mouse model of systemic fungal infection. Unlike the vast majority of mutants with defects in this bloodstream infection model (Noble et al., 2010), strains that lack *LIP2* undergo normal yeast-to-hypha morphogenesis, the best-studied virulence attribute of this pathogen. Rather, infection with a *lip2* null mutant triggers an exaggerated IL-17A immune response in infected kidneys, which is followed by rapid fungal clearance and survival of the host. Virulence of the *lip2* mutant is fully restored in *Il17af*$^{-/-}$ animals that fail to produce IL-17A and IL-17F, suggesting that IL-17 may play an unanticipated role in promoting fungal clearance from systemically infected animals. Using flow cytometry, we discovered that IL-17A production is induced in renal TCR$\gamma\delta$+ T cells within 6 h of systemic infection with *C. albicans*, especially the *lip2* mutant. Moreover, IL-23, which is known to stimulate IL-17 expression by TCR$\gamma\delta$+ T cells (Sutton et al., 2009), is upregulated in renal dendritic cells (DCs) with similar kinetics. To test the hypothesis that DCs are directly activated by exposure to *C. albicans*, we performed *in vitro* coculture experiments with bone-marrow-derived DCs (BMDCs). Unlike wild-type (WT) *C. albicans* or a *lip2+LIP2*-complemented strain, the *lip2* null mutant and strains expressing catalytically inactive variants of Lip2 trigger IL-23A secretion into culture supernatants. Strikingly, fungal activation of BMDCs is inhibited in the presence of 0.1 μM palmitic acid, a product of Lip2 lipase activity. These findings support a model in which *C. albicans* utilizes Lip2 to modify the lipid milieu of infected organs during systemic infection, thereby inhibiting the activation of tissue-resident DCs and preventing an IL-17-dependent antifungal immune response.

RESULTS

Lip2 is critical for *C. albicans* pathogenicity during systemic infection

We identified Lip2 as a candidate fungal virulence factor in a competitive screen of ~1,500 *C. albicans* GRACE (gene replacement and conditional expression) mutants (Roemer et al., 2003) in a mouse model of bloodstream infection (P.B. et al., unpublished data). Each barcoded GRACE strain contains one null allele of a specific open reading frame (ORF), as well as an intact copy of the ORF, whose expression is controlled by a doxycycline (DOX)-repressible promoter; note that the *C. albicans* genome is diploid. Strains were propagated individually in the presence of DOX (0.1 mM DOX in liquid yeast extract peptone dextrose medium [YEPD]), followed by pooling of up to 96 strains into 20 mixed inocula. 5×10^5 colony-forming units (CFUs) of each inoculum was introduced into 5 BALB/c mice by retro-orbital injection, and an aliquot was plated onto Sabouraud agar (with ampicillin and gentamicin) as the "inoculum" sample. Infected animals were maintained on DOX-containing drinking water (0.25 mg/mL) until they developed clinical morbidity criteria (body condition score $\leq$ 2, respiratory distress, and/or immobility), typically after 5–7 days of systemic infection. Kidneys (the primary target organ in this infection model) from each euthanized animal were homogenized and plated onto Sabouraud agar (with ampicillin and gentamicin) as "recovered" samples. Finally, genomic DNA from the inoculum and recovered samples was used to generate barcode sequencing libraries, and relative strain abundance was determined by Illumina sequencing, as previously described (O'Meara et al., 2015). The competitive index (CI) of each mutant in a given animal was calculated as the $\log_2$ function of its relative abundance in the recovered pool compared with its relative abundance in the inoculum.

The *lip2*$^{DOX\text{-}OFF}$ mutant was one of the first loss-of-fitness mutants to be identified in the virulence screen; comprehensive results for additional virulence mutants as well as strains identified in a parallel screen for gut commensalism factors will be reported separately (P.B. et al., unpublished data). To validate the virulence defect of *lip2*$^{DOX\text{-}OFF}$, we retested the GRACE strain in 1:1 competition against WT *C. albicans* in the presence of DOX. As shown in Figure 1A, *lip2*$^{DOX\text{-}OFF}$ was strongly outcompeted by WT in kidneys of all five systemically infected animals, similar to results obtained in the primary screen. We next compared two independent *lip2* null mutants, which were constructed in a different strain background (SN152), to an isogenic WT strain and a *lip2+LIP2* gene addback strain in monotypic (single strain) infections. As shown in Figure 1B, both *lip2* mutants exhibited significantly reduced lethality compared with the WT and complemented strains (Figure 1B). These results establish that *LIP2* is required for virulence during systemic infection.

The best-known virulence attribute of *C. albicans* is its ability to transition from single-celled budding yeast into elongated, multicellular hyphae (Noble et al., 2017). Unlike yeast, hyphae are naturally invasive and express virulence factors such as adhesins, tissue-degrading enzymes, and the secreted toxin candidalysin (Noble et al., 2017). The vast majority of published *C. albicans* virulence mutants exhibit defects in yeast-to-hypha morphogenesis (Noble et al., 2010). To determine whether *LIP2* is required for hypha formation, *lip2* and WT strains were profiled under multiple *in vitro* hypha-inducing conditions. As shown in Figure S1A, *lip2* and WT exhibited equivalent patterns of filamentation in the "germ tube" clinical diagnostic assay, as well as in YEPD + 5% serum, Spider, and RPMI media maintained at 37°C. Likewise, germination rates for *lip2* and WT were similar throughout a 180-min time course (Figure S1B). These results suggest that *LIP2* is dispensable for morphogenesis. Exposure of WT *C. albicans* to hypha-promoting *in vitro* culture conditions results in upregulation of *LIP2* gene expression (by RT-qPCR, Figure S1C), suggesting that it may encode a hypha-specific virulence factor.

To further characterize the virulence defect of the *lip2* null mutant, we performed a series of monotypic, timed infections with *lip2*, WT, or saline (mock infection); the *lip2+LIP2* strain was also tested in a subset of animals. Three BALB/c mice per comparison group were euthanized after 1, 4, 6, 16, 24, 48, 72, 96, 120, and 144 h of systemic infection, followed by analysis of kidneys for fungal burden, pattern of fungal invasion, tissue

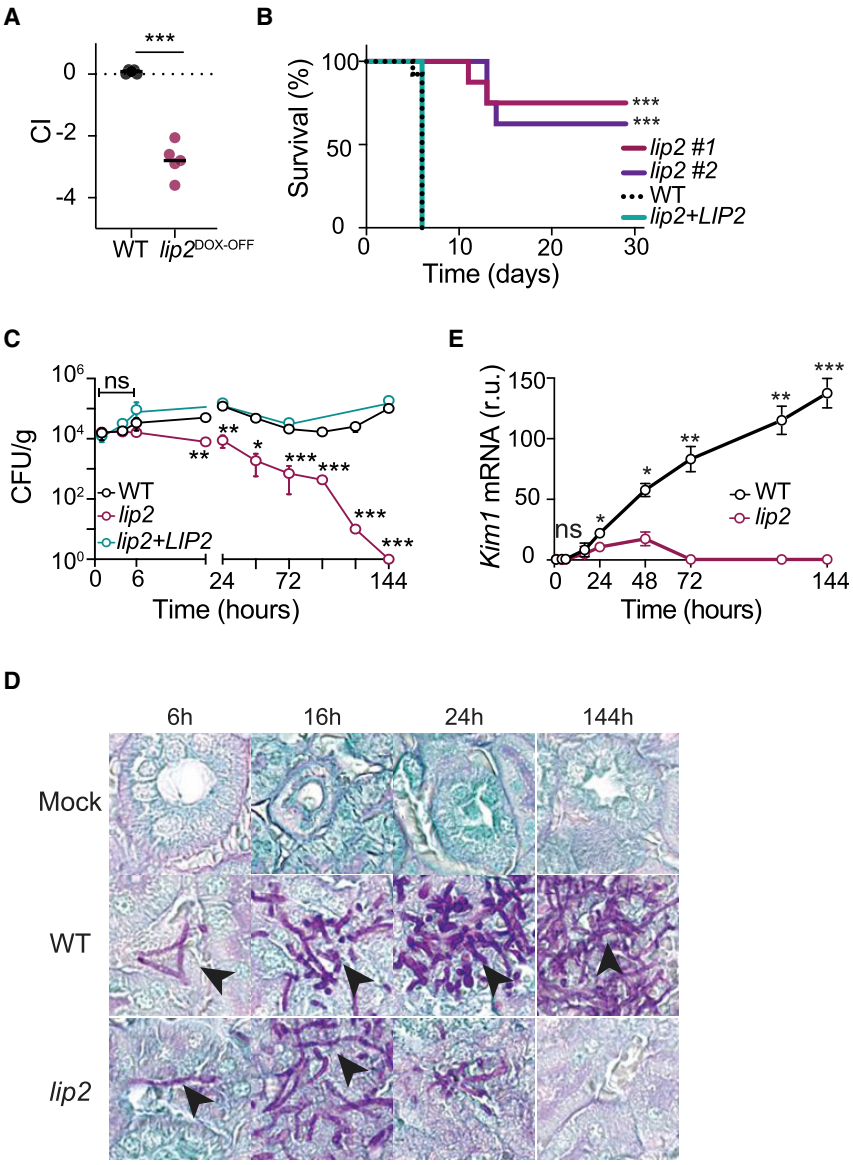

Figure 1. Lip2 is required for pathogenicity

(A) *lip2*$^{DOX-OFF}$ is defective for systemic virulence in the presence of doxycycline. Female BALB/c mice were treated with 0.25 mg/mL doxycycline via drinking water for 7 days prior to retro-orbital injection with 1 × 10^5 CFU of a 1:1 mixture of WT and *lip2*$^{DOX-OFF}$; relative strain abundance in kidneys was determined using qPCR. Statistical significance was determined by a paired two-tailed t test; ***p < 0.001.

(B) *lip2* mutants exhibit reduced lethality compared with WT or a *lip2+LIP2* gene addback strain. Groups of female BALB/c mice were injected with 1 × 10^5 CFU WT (n = 16), *lip2* (isolate 1, n = 8), *lip2* (isolate 2, n = 8), or *lip2+LIP2* (n = 8). Statistical significance between WT and *lip2* #1 *or lip2* #2 was determined by Mantel-Cox test; ***p < 0.001.

(C) *lip2* fails to persist in infected kidneys. Groups of female BALB/c mice were infected with 1 × 10^5 CFU of WT, *lip2*, or *lip2+LIP2*, followed by euthanasia of three animals per group at the indicated time points. CFUs were determined by plating right kidney homogenates onto Sabouraud agar (supplemented gentamicin and ampicillin) and counting after 2 days. Data represent the mean and standard deviations. Statistical significance between WT and *lip2* was determined by an unpaired two-tailed t test; ns, nonsignificant, **p < 0.01; ***p < 0.001. (Note that points without visible error bars displayed SEMs smaller than the circle.)

(D) *lip2* forms normal-appearing hyphae in host kidneys. 400× image of PAS-stained left kidneys from experiment described in (C).

(E) *lip2* causes minimal damage to kidneys. *Kim1* mRNA was measured in the right kidney homogenates and normalized to *Gadph*. Statistical significance was determined by an unpaired two-tailed t test; *p < 0.05, **p < 0.01, ***p < 0.001, ****p < 0.0001. (Note that points without visible error bars displayed SEMs smaller than the circle.)

damage, and expression of selected host transcripts. As shown in Figure 1C, *lip2*, WT, and *lip2+LIP2* were equally represented in kidneys (~10^4 CFU/g) after 1, 4, and 6 h of infection. By 18 h, however, the burden of *lip2* was significantly reduced compared with the other two strains. Whereas titers of WT and the *lip2+LIP2* strain remained relatively stable (~10^4–10^5 CFU/g kidney) throughout the infectious time course, titers of *lip2* progressively declined until becoming undetectable at 144 h. Fungal titers were also determined in the liver and spleen at selected time points (Figure S2A). The three fungal strains exhibited similar abundances (~10^3 CFU/g) in both organs after 1 h. In the liver, titers of WT and *lip2+LIP2* remained relatively stable throughout the time course, but *lip2* became undetectable by 144 h. In contrast, all three fungal strains were rapidly cleared from the spleen. This analysis indicates that *LIP2* is not necessary for the initial entry of *C. albicans* into solid organs, but it is required for the maintenance of a stable infection in the kidney and liver.

Patterns of fungal invasion were assessed in sectioned left kidneys after staining with periodic acid Schiff (PAS). As shown in Figures 1D and S2B, *lip2* formed normal-appearing hyphae in kidneys, suggesting that *lip2* is competent for morphogenesis in the host as well as under *in vitro* conditions (Figures S1A and S1B). However, stark differences were apparent in the extent of renal invasion by *lip2* versus WT. By 16 h, large clusters of WT hyphae could be visualized throughout the renal cortex (Figure S2C), a highly perfused region that receives ~25% of cardiac output (Lionakis et al., 2011; Rajendran et al., 2013). Over the remainder of the time course, the areas infiltrated by WT *C. albicans* enlarged and coalesced until, by 144 h, they spanned the renal cortex, corticomedullary junction, and portions of the medulla. In contrast, *lip2* formed much smaller collections within the renal cortex at 16 h (Figures S2B and S2C), and these areas diminished in size over subsequent time points, becoming virtually undetectable by 144 h.

Kidney damage was evaluated histologically on hematoxylin and eosin (H&E)-stained left kidney sections. Starting at 16 h, WT-infected kidneys exhibited areas of tissue necrosis with

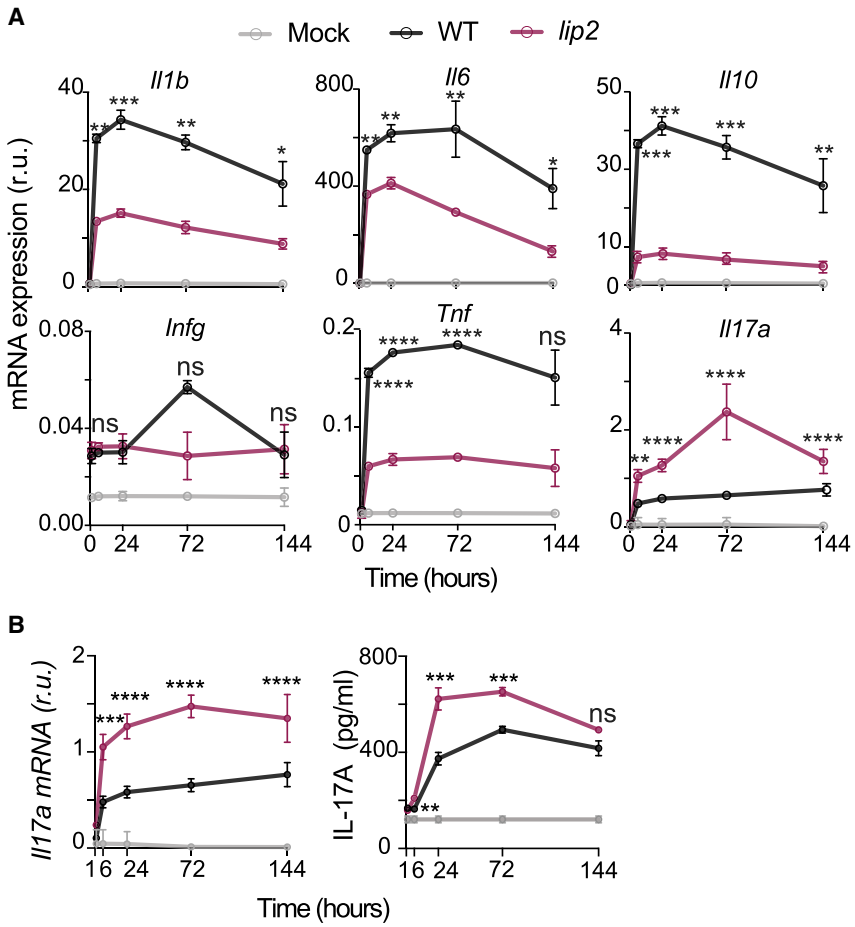

Figure 2. *lip2* induces an elevated IL-17 response in kidneys

(A) *lip2* provokes an exaggerated *Il17a* response in infected kidneys. Groups of female BALB/c mice were infected with 1 × 10^5 CFU of WT or *lip2*, followed by euthanasia of three animals per group at the indicated time points. *Il1b*, *Il6*, *Il10*, *Ifng, Tnf*, *Il17a* mRNA expression was assessed by RT-qPCR of RNA recovered from kidney homogenates (expression relative to *Gadph*). Statistical significance of differences between WT-infected kidneys and *lip2*-infected kidneys was determined by an unpaired two-tailed t test; *p < 0.05, **p < 0.01, ***p < 0.001, ****p < 0.0001. (Note that points without visible error bars displayed SEMs smaller than the circle.)

(B) *lip2* induces a strong renal IL-17A response during systemic infection. Groups of BALB/c mice were infected with 1 × 10^5 CFU WT or *lip2* followed by euthanasia of three animals per group at the indicated time points. *Il17a* mRNA was measured by RT-qPCR in the right kidney homogenates and normalized to *Gadph* (left panel). IL-17A protein production was evaluated by ELISA in the left kidney homogenates (right panel). Statistical significance between WT and *lip2* was determined by an unpaired two-tailed t test; ns: p = 0.1797; **p < 0.01; ***p < 0.001; ****p < 0.0001.

microabscess formation at the sites of hyphal infiltration in the renal cortex (Figure S2D). These areas of injury expanded and progressed over the subsequent time course, resulting in interstitial edema, widespread acute tubular injury and parenchymal necrosis, and frank hemorrhage. By contrast, *lip2*-infected organs remained free of significant injury throughout the time course, despite the presence of localized microabscesses in the cortex that peaked at 24 h and subsequently resolved (Figure S2D). We next used RT-qPCR to evaluate right kidney homogenates for *Kim1* (kidney injury molecule-1) mRNA, a highly sensitive marker of acute renal injury (Bonventre, 2014). As shown in Figure 1E, during infection with WT *C. albicans*, renal *Kim1* levels were elevated throughout the time course and progressively increased until the end of observation at 144 h. By comparison, *Kim1* was briefly elevated at 24 and 48 h in *lip2*-infected organs, albeit to levels that were significantly lower than in WT-infected organs, followed by a return to baseline at subsequent time points (Figure 1E). These results indicate that, consistent with its reduced titers and lesser degree of renal infiltration after ~24 h, *lip2* causes only minor, transient injury to the host.

IL-17 triggers an antifungal immune response during invasive candidiasis

We considered two potential explanations for the persistence defect of *lip2* in infected organs: the encoded lipase may be required for fungal proliferation, for example, because of its role in nutrient acquisition, or it may defend against clearance by the host. To gauge the host immune response to *lip2* versus WT strains in infected kidneys, we quantified transcript levels for six pro-inflammatory cytokines in whole kidney homogenates using RT-qPCR. As shown in Figure 2A, expression of *Il1β, Il6, Il10*, and *Tnf* was significantly higher in kidneys infected with WT compared with *lip2*, whereas *Ifng* was minimally induced by either strain. *Il17a* was the only cytokine to be expressed more strongly in *lip2*-infected organs, as early as 6 h after infection. The latter result was confirmed in additional animals, confirming elevation of *Il17a* mRNA and, following a delay, IL-17A protein in kidneys infected with *lip2* (Figure 2B).

We reasoned that, if IL-17 plays an important role in eliminating *lip2* from infected kidneys, then the virulence defect of the mutant may be suppressed in animals that fail to produce IL-17. Consistent with this prediction, *lip2* exhibited normal competitive fitness with WT *C. albicans* in *Il17af*$^{-/-}$ mice, in contrast to the strong competitive defect observed in WT (*Il17af*$^{+/+}$) littermate control animals (Figure 3A). Similarly, *lip2* demonstrated similar lethality to that of WT *C. albicans* in monotypic infections of *Il17af*$^{-/-}$ mice, whereas the same dose of the mutant provoked no mortality in WT (*Il17af*$^{+/+}$) littermates (Figure 3B). We confirmed that *lip2* triggers elevated levels of *Il17a* RNA and IL-17A protein in the kidneys of C57B/6J mice (the genetic background of *Il17af*$^{-/-}$ animals; Figure S3A) as previously observed in BALB/c mice (Figure 2B). To determine the impact of IL-17 on fungal clearance from infected internal organs, we compared fungal titers in kidneys of *Il17af*$^{-/-}$ versus WT

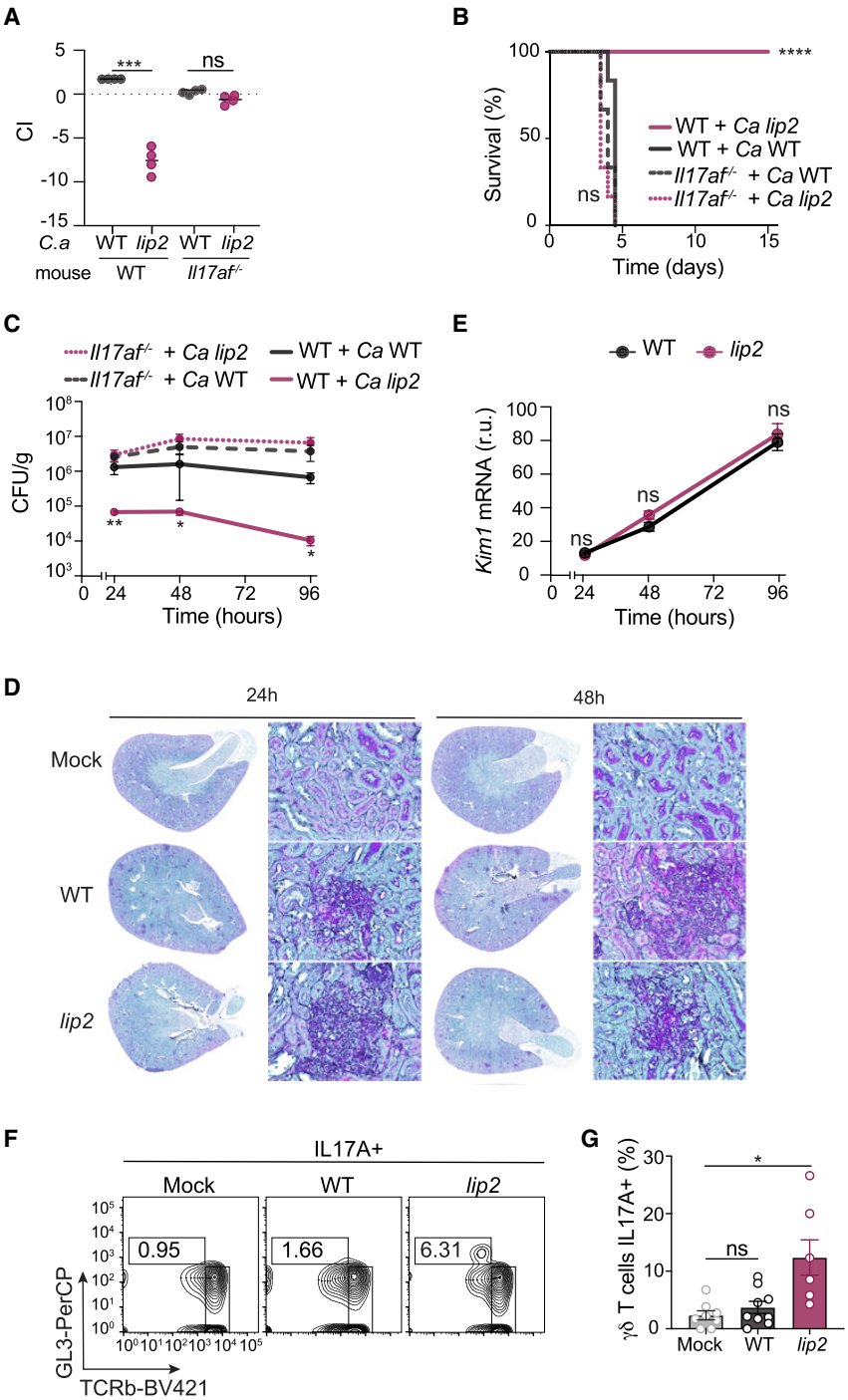

Figure 3. IL-17 mediates an antifungal response during systemic infection

(A) Competitive fitness of *lip2* is restored in *Il17af*$^{-/-}$ mice. Groups of four (male and female) WT or *Il17af*$^{-/-}$ C57BL/6J mice were systemically infected with 5 × 10^5 CFU of a 1:1 mixture of WT and *lip2*. Mice were euthanized after 4 days and relative strain abundance in kidneys was determined using qPCR. Statistical significance between WT and *lip2* was determined by a paired two-tailed t test; ns: p = 0.0685; ***p < 0.001.

(B) Virulence of *lip2* in monotypic infections is restored in *Il17af*$^{-/-}$ mice. Groups of WT or *Il17af*$^{-/-}$ C57BL/6 (male and female) mice were systemically infected with 5 × 10^5 CFU of WT or *lip2* (n = 8 per group). Statistical significance between WT and *lip2* was determined by the Mantel-Cox test; ***p < 0.001.

(C) Clearance of *lip2* from kidneys requires IL-17. Groups of three WT or *Il17af*$^{-/-}$ C57BL/6J (male and female) mice were infected with 5 × 10^5 CFU of WT or *lip2*. Animals were euthanized after 24, 48, or 96 h, and the fungal burden in kidneys was determined by plating right kidney homogenates onto Sabouraud agar (supplemented with gentamicin and ampicillin). Statistical significance was determined by one-way ANOVA (Tukey's multiple comparisons test); *p < 0.05, **p < 0.01.

(D) *lip2* and WT *C. albicans* induce similar amounts of renal damage in *Il17af*$^{-/-}$ C57BL/6J mice (male and female were used). 400× image of PAS-stained left kidneys from the experiment described in (C).

(E) *Kim1* mRNA levels in *Il17af*$^{-/-}$ C57BL/6J animals infected with *lip2* or WT *C. albicans*. RT-qPCR was used to quantify *Kim1* mRNA in right kidney homogenates, and results were normalized to *Gadph*. Statistical significance was determined by an unpaired two-tailed t test ns: p = 0.6130. (Note that points without visible error bars displayed SEMs smaller than the circle.)

(F and G) Representative flow cytometry plots and quantification of renal TCRγδ+ T cells producing IL-17A upon infection with *lip2*. Groups of C57BL/6J (male and female) mice were infected with 1 × 10^6 CFU of WT or *lip2*. Animals were euthanized after 6 h. Flow cytometry was performed on total renal cells after 4 h of stimulation with PMA, ionomycin, and Golgi STOP. (F) Flow cytometry plots for IL17A+ TCRγδ+ cells for one animal from each group (see Figure S3C for complete FACS gating). (G) Percentage of renal TCRγδ+ T cells producing IL-17A from *C. albicans*-infected kidneys (gated on live CD45$^+$ cells). Statistical significance was determined by one-way ANOVA (Tukey's multiple comparisons test); ** p < 0.01.

(*Il17af*$^{+/+}$) animals infected with *lip2* or WT *C. albicans*. As shown in Figure 3C, *lip2* and WT strains exhibited nearly identical abundance (~10^7 CFU/g kidney) in kidneys of *Il17af*$^{-/-}$ animals throughout a 96-h time course, whereas the *lip2* null mutant was substantially depleted at all monitored time points in WT mice. Analysis of renal histology (Figure 3D) and *Kim1* mRNA levels (Figure 3E) in infected kidneys revealed that the defects of the *lip2* strain in deep organ penetration and kidney damage are also suppressed in *Il17af*$^{-/-}$ animals. Finally, using RT-qPCR to evaluate the expression of multiple cytokines (IL-1β, IL-6, IL-10, and IFNγ) in infected kidneys, we confirmed that *lip2* and WT *C. albicans* elicit similar cytokine responses in *Il17af*$^{-/-}$ animals (Figure S3B). These results argue that host expression of IL-17 is required for the observed fitness defects of *C. albicans lip2* in a mouse model of invasive infection. Conversely, the enhanced virulence of *lip2* in *Il17af*$^{-/-}$ animals suggests that IL-17 plays an important role in defending WT animals from systemic fungal infection.

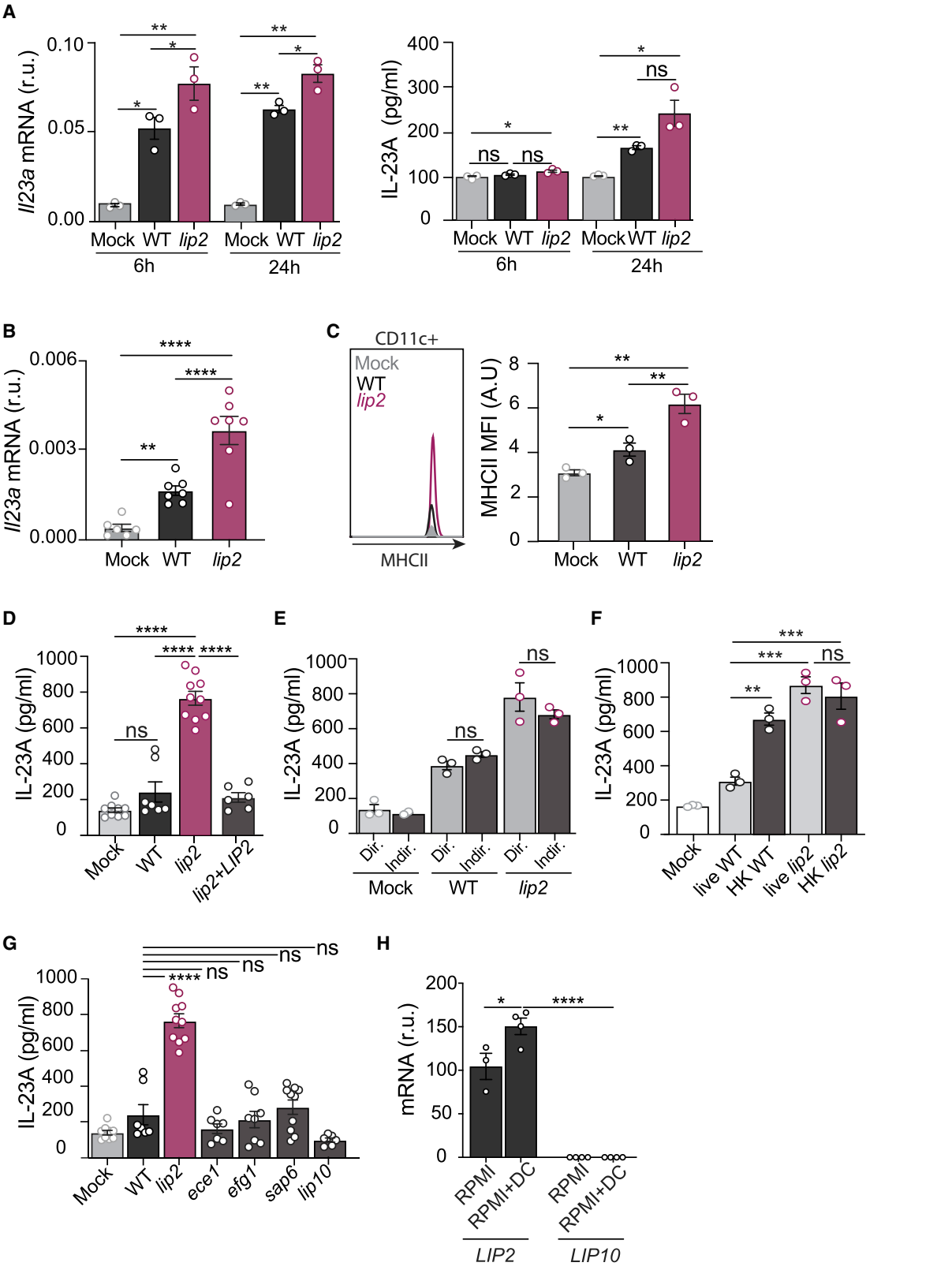

(legend on next page)

To probe the mechanism by which Lip2 modulates host immunity, we began by asking which cells produce IL-17 in infected kidneys. Th17 cells are generally considered to be a major source of IL-17 in mammals (Huppler et al., 2012; Sparber and LeibundGut-Landmann, 2019), and this cell type has previously been shown to protect against systemic candidiasis in mice that have been intestinally colonized with *C. albicans* (Shao et al., 2019). However, $CD4^+$ T cells are poorly represented in mouse kidneys during the first 24 h of *C. albicans* bloodstream infection (Lionakis et al., 2011), whereas we observe increases in renal *Il17a* mRNA within 6 h (Figures 2A and 2B). We therefore focused on tissue-resident immune cells that are capable of producing IL-17, such as natural killer T cells (NKTs), innate lymphoid cells (ILCs), and TCR$\gamma\delta$+ T cells; note that TCR$\gamma\delta$+ T cells have previously been reported to produce IL-17 in kidneys during systemic candidiasis (Ramani et al., 2016). Kidneys were recovered from C57B/6J mice 6 and 24 h after inoculation with the *lip2* mutant, WT, or normal saline (''mock'' infection), followed by cell dissociation and staining for intracellular IL-17A and leukocyte surface markers. As shown in Figures 3F, 3G, and S3C, TCR$\gamma\delta$+ T cells (but not ILC3s or $CD4^+$ T cells) were identified as a major source of IL-17 in *lip2*-infected kidneys. Similar results were obtained using SMART17A mice (in the C57B/6J background) that display a human low-affinity nerve growth factor receptor marker on the surface of cells that express mouse *Il17a* (Figure S3D) (Price et al., 2012).

Lip2 suppresses the activation of renal dendritic cells

Because TCR$\gamma\delta$+ T cells typically upregulate IL-17 in response to an upstream cytokine, such as IL-23 (Sparber and LeibundGut-Landmann, 2019), we investigated the expression of *Il23* in infected kidneys. As shown in Figure 4A, renal *Il23* mRNA was significantly elevated within 6 h of infection with WT *C. albicans*, and the effect was even stronger in *lip2*-infected organs. A similar pattern was observed with IL-23 protein, following a delay (Figure 4A). Macrophages and DCs are common sources of IL-23 in solid organs. Using flow cytometry, DCs and macrophages were quantified in kidneys recovered after 6 h of infection by WT or *lip2*, or in mock-infected mice. As shown in Figure S4A–S4D, DCs were found to compose ~15% of total renal $CD45^+$ cells, regardless of infection with *C. albicans*, whereas the macrophage population was too small to measure with accuracy; note that these findings are consistent with a previous report (Lionakis et al., 2011). Using RT-qPCR to quantify *Il23 mRNA* expression in isolated renal DCs, we observed significant upregulation after 6 h of infection with WT *C. albicans* and an even stronger response to the *lip2* strain (Figure 4B). In support of DC activation by *C. albicans*, flow cytometry revealed stepwise increases in surface expression of MHCII in DCs from organs infected with WT or *lip2* (Figure 4C). Together, these results suggest that tissue-resident DCs respond to fungal invasion of the kidney by producing IL-23, a known activator of IL-17 expression. For reasons that remain unclear, this response is exaggerated in the presence of *lip2*.

To test whether *C. albicans* can directly activate IL-23 production by DCs, coculture experiments were performed with BMDCs prepared from C57B/6J mice. BMDCs were incubated at an MOI of 1 with WT, *lip2*, a *lip2+LIP2* complemented strain, or cell medium alone (mock) for 2 h, followed by quantitation of IL-23 in the culture supernatants. As shown in Figure 4D, exposure to *lip2*, but not WT or *lip2+LIP2*, induced a strong IL-23 response from cocultured BMDCs. To determine whether direct cell-cell contact is required for BMDC activation by *C. albicans*, we repeated the experiment, this time varying whether cells were mixed directly in the same wells (Dir) or indirectly (Indir) in compartments separated by a

Figure 4. Lip2 suppresses the activation of renal dendritic cells

(A) *lip2* induces IL-23A production in kidneys. Groups of female C57BL/6J mice were infected with 1×10^6 CFU of WT or *lip2* followed by euthanasia of three animals per group at the indicated time points. *Il23a* mRNA was measured by RT-qPCR in right kidney homogenates and normalized to *Gadph* (left panel). IL-23A protein production was evaluated by ELISA in the left kidney homogenates (right panel). Statistical significance was determined by one-way ANOVA (Tukey's multiple comparisons test); *p < 0.05; **p < 0.01.

(B) Kidney resident DCs respond to *C. albicans* invasion. Groups of C57BL/6J mice were infected 1×10^6 CFU of WT or *lip2* for 6 h. Renal DCs were isolated and *Il23a* mRNA levels were measured by RT-qPCR and normalized to *Gadph*. Statistical significance was determined by one-way ANOVA (Tukey's multiple comparisons test); **p < 0.01; ***p < 0.001; ****p < 0.0001.

(C) Infection with *lip2* is associated with increased cell surface expression of MCHII by renal DCs. Groups of C57BL/6J mice were infected 1×10^6 CFU of WT or *lip2* for 6 h. DCs were analyzed by flow cytometry for MCHII. Statistical significance was determined by one-way ANOVA (Tukey's multiple comparisons test); *p < 0.05; **p < 0.01.

(D) *lip2* stimulates IL-23 production by BMDCs. BMDCs from C57BL/6J mice were cultured with WT, *lip2*, or *lip2+LIP2* at a multiplicity of infecction (MOI) of 1 for 2 h followed by measurement of IL-23A in cell supernatants by ELISA. Statistical significance was determined by one-way ANOVA (Tukey's multiple comparisons test); ns: p = 0.6247; ****p < 0.0001.

(E) *lip2*-stimulated activation of BMDCs does not require cell-cell contact. BMDCs from C57BL/6J mice were cultured in the same well with WT or *lip2* (Dir), or separately using a transwell system (Indir) at an MOI of 1 for 2 h followed by measurement of IL-23A in cell supernatants by ELISA. Statistical significance between direct versus indirect contact with WT or *lip2* was determined by an unpaired two-tailed t test; ns: p = 0.6247.

(F) Cell viability is required to repress BMDC activation. BMDCs from C57BL/6J mice were cocultured with live or heat-killed (HK) forms of WT or *lip2* at an MOI of 1 for 2 h followed by measurement of IL-23A in cell supernatants by ELISA. Statistical significance between the different groups was determined by one-way ANOVA (Tukey's multiple comparisons test); ns: p > 0.5, **p < 0.01, ***p < 0.001.

(G) The ability to activate BMDCs is specific to *lip2*. Coculture assays were performed with *lip2*, three other virulence-defective mutants (*efg1, ece1, sap6*), and *lip2* (*lip10*) as described in (D). Statistical significance between WT and the different mutants was determined by one-way ANOVA (Tukey's multiple comparisons test); ns WT versus *ece1*: 0.8937; ns WT versus *efg1*: 0.9999, ns WT versus *sap6*: 0.9977, ns WT versus *lip10*: 0.3074: WT versus *lip2*: ****p < 0.0001.

(H) *LIP2* but not *LIP10* is expressed under co-coculture conditions. WT *C. albicans* was propagated alone or in coculture with BMDCs for 2 h, followed by assessment of *LIP2 and LIP10* mRNAs by RT-qPCR; reported values were normalized to *ACT1*. Statistical significance between RPMI and RPMI + DC was determined by an unpaired two-tailed t test; *p < 0.05, ****p < 0.0001.

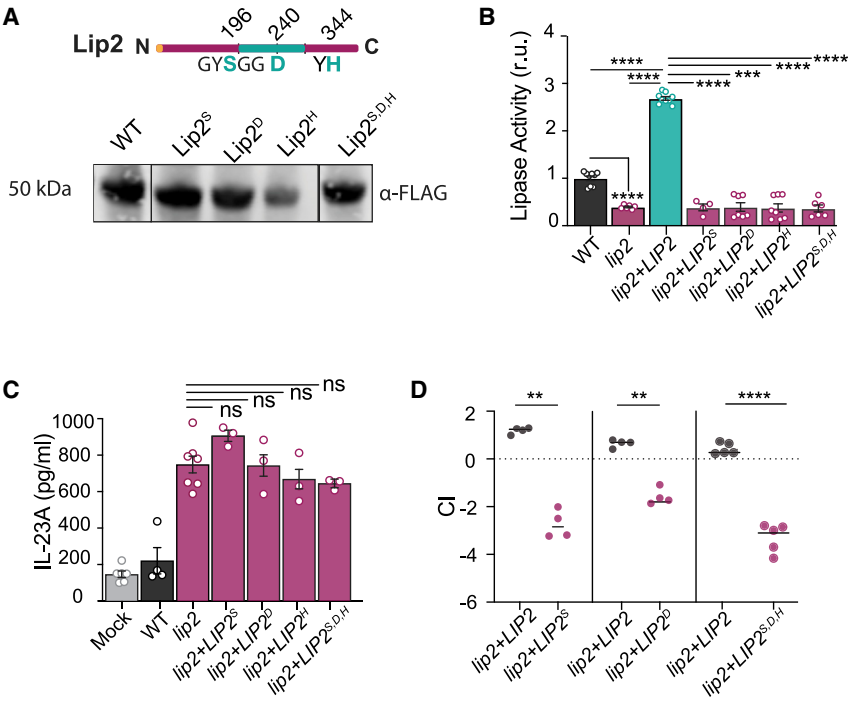

Figure 5. Predicted catalytic residues of Lip2 is required for its immunomodulatory role

(A) Lip2 point mutant proteins are expressed. Cartoon of Lip2 protein domains (top). The lipase domain is represented by the green central region, with targeted residues of the predicted catalytic site also colored green. Immunoblot (bottom) of WT and point mutant alleles recovered from cell culture supernatants. Lip2 proteins are fused at the C terminus to 6-His-FLAG (HHHHHHGGDYKDDDDK) and immunoblots were probed with anti-FLAG.

(B) Lip2 point mutants exhibit reduced lipase activity. Strains expressing the indicated allele of *LIP2* were propagated to mid log growth (OD_{600} = 1) in liquid YEPD. Lipase assays were performed following a 10-min incubation of supernatants with mixed lipids. Statistical significance between the different groups was determined by one-way ANOVA (Tukey's multiple comparisons test); ***p < 0.001, ****p < 0.0001.

(C) Lip2 lipase activity is required to suppress the activation of BMDCs by *C. albicans*. Coculture assays were performed with yeasts expressing WT Lip2 or the indicated Lip2 point mutants as in Figure 4D. Statistical significance between *lip2* and the point-mutation mutants was determined by one-way ANOVA (Tukey's multiple comparisons test); ns: p = 0.1964.

(D) Lip2 lipase activity is required for virulence. BALB/c mice were infected with 1 × 10^5 CFU of a 1:1 mixture between *lip2+LIP2* and either *lip2+LIP2*^{S196A}, *lip2+LIP2*^{D240A}, or *lip2+LIP2*^{S196A,D240A,H344A}. Relative strain abundance in kidneys was determined by qPCR. Statistical significance between *lip2+LIP2* and mutants was determined by a paired two-tailed t test; **p < 0.01, ****p < 0.0001.

porous membrane. As shown in Figure 4E, *C. albicans* triggered similar IL-23 responses from BMDCs regardless of whether the cells were in direct physical contact, suggesting that a soluble fungal signal may be responsible for the activation of BMDCs. Finally, we asked whether cell viability is required for the ability of WT *C. albicans* to suppress activation of BMDCs. As shown in Figure 4F, coincubation of BMDCs with heat-killed (HK) but not viable (live) WT *C. albicans* resulted in the secretion of IL-23, similar to the effect of coincubation with live or HK *lip2*. Together, these results suggest that a soluble fungal signal can activate IL-23 production by BMDCs, but live yeasts are able to block immune activation in a *LIP2*-dependent fashion.

To determine whether BMDC activation is specific to *lip2*, we tested three additional virulence mutants and a mutant defective in the closest paralog to Lip2 in the coculture assay. As shown in Figure 4G, coculture of BMDCs with mutants defective in candidalysin production (*ece1*) (Moyes et al., 2016), yeast-to-hypha morphogenesis (*efg1*) (Stoldt et al., 1997), a secreted aspartyl protease (*sap6*) (Jackson et al., 2007), or Lip10 (*lip10*) failed to elicit IL-23 production beyond the level observed during coculture with WT. In contrast to *LIP2, ECE1, EFG1*, and *SAP6* (Figure S4E), *LIP10* is not detectably expressed by WT *C. albicans* under the coculture assay conditions (Figures 4H and S4E); therefore, the lack of a *lip10* phenotype may reflect the absence of gene expression rather than a lack of immunomodulatory activity of the encoded enzyme. This caveat notwithstanding, the ability to activate BMDCs in the coculture assay appears to be unique to *lip2*, raising the possibility that the virulence-promoting activity of Lip2 is to dampen immune activation of tissue-resident DCs in kidneys and other infected organs.

Lipase activity is required for the immunomodulatory role of Lip2

LIP2 encodes a secreted lipase with nine paralogs in *C. albicans* (Hube et al., 2000). To determine whether lipase activity is required for the immune dampening function of Lip2, we engineered four *LIP2* point mutants (*lip2*^{S196A}, *lip2*^{D240A}, *lip2*^{H344A}, and *lip2*^{S196A,D240A,H344A}) that target conserved residues in the predicted lipase domain (Figure 5A). FLAG-tagged versions of each mutant allele and WT *LIP2* were individually introduced into a *lip2* null strain, and protein expression and secretion were confirmed by immunoblotting of the respective cell supernatants with anti-FLAG antibodies (Figure 5A). Cell supernatants from the point mutant strains were next assessed for *in vitro* lipase activity. Compared with WT *C. albicans* or *lip2+LIP2*, significantly reduced lipase activity was associated with the point mutant strains, similar to *lip2* null mutant (Figure 5B), suggesting that the encoded proteins are catalytically inactive. Further, in coculture assays with BMDCs, all four-point mutant strains activated IL-23 production to a similar degree as *lip2* (Figure 5C). Finally, the competitive fitness of the *lip2+LIP2*^{S196A}, *lip2+LIP2*^{D240A}, and lip2+*LIP2*^{S196A,D240A,H344A} strains was assessed in 1:1 competitions against WT in the mouse systemic infection model. All three mutants exhibited significantly reduced fitness in the kidneys (Figure 5D), similar to the phenotype of *lip2*. Together, these experiments suggest that the lipase activity of Lip2 is required for suppression of the BMDC response to *C. albicans* and for virulence in the host.

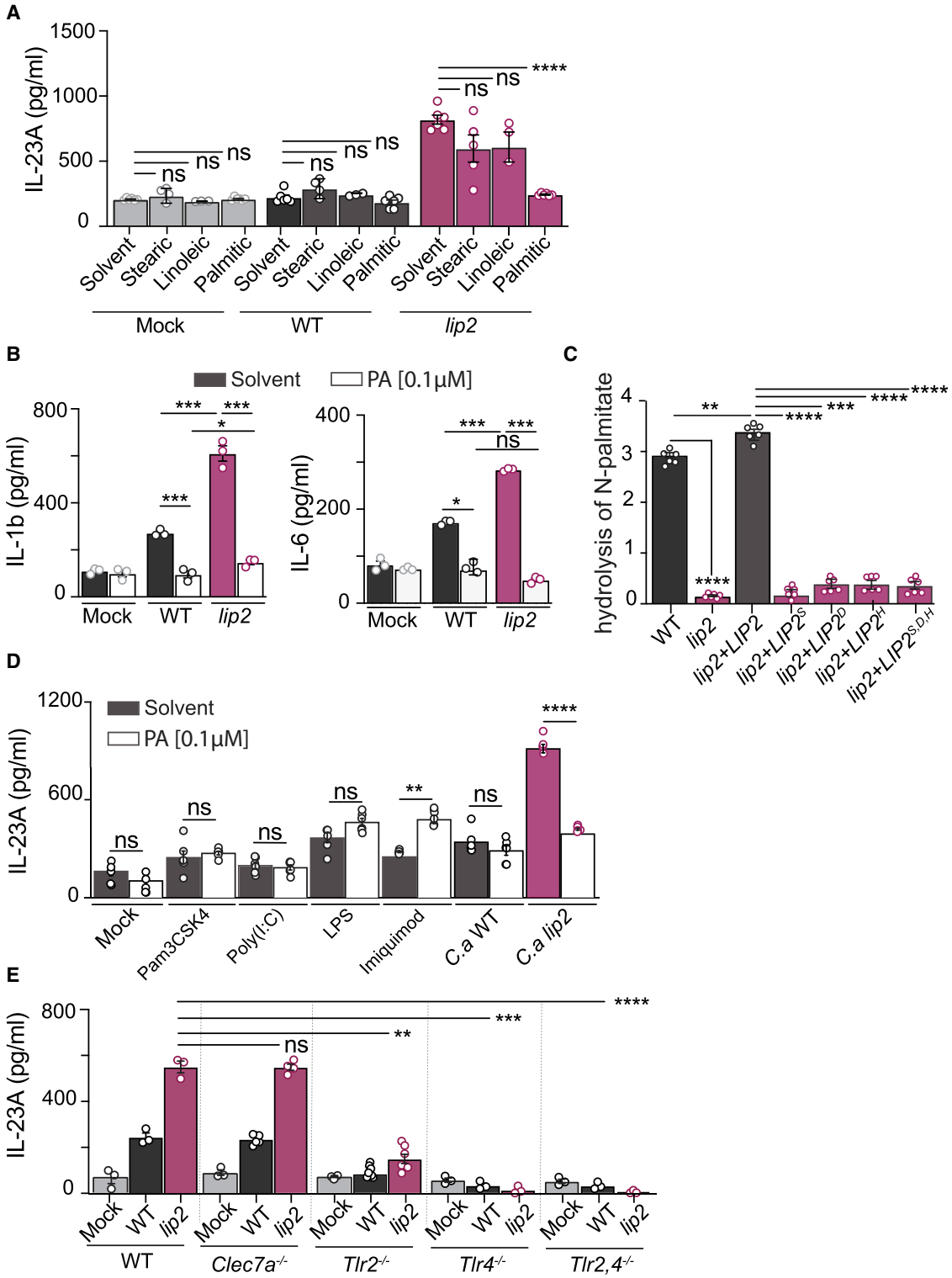

Figure 6. The immune dampening defect of *lip2* is complemented by palmitic acid

(A) Palmitic acid suppresses the IL-23 response of BMDCs to *C. albicans*. BMDCs from C57BL/6J mice were incubated with 0.1 μM of fatty acids (palmitic acid, stearic acid, or linoleic acid) or solvent alone (chloroform), with or without WT *C. albicans* or *lip2* at an MOI of 1 for 2 h, followed by measurement of IL-23A in cell supernatants by ELISA. Statistical significance between solvent control and fatty acid was determined by one-way ANOVA (Tukey's multiple comparisons test); ns: $p > 0.05$, ****$p < 0.0001$.

(legend continued on next page)

Palmitic acid suppresses the activation of dendritic cells

Lipases are enzymes that catalyze the hydrolysis of triglycerides to fatty acids and glycerol. We hypothesized that, within the host, Lip2 may modulate DC reactivity by increasing the local concentration of one or more fatty acids. To test this hypothesis, we assayed the ability of several common fatty acids to suppress IL-23 production by BMDCs exposed to *lip2*. As shown in Figures 6A, S5A, and S5B, 0.1 μM palmitic acid—but not stearic acid, linoleic acid, or solvent alone—suppressed the IL-23 response of BMDCs to *lip2* to the level observed in unexposed BMDCs (or WT-exposed BMDCs). In addition to IL-23, cytokines such as IL-1β and IL-6 are capable of driving IL-17 production by TCRγδ+ T cells. To determine whether palmitic acid affects the production of IL-1β and/or IL-6 following exposure of BMDCs to *C. albicans*, we assessed the levels of these cytokines following 2-h coculture experiments performed in the presence or absence of palmitic acid. Interestingly, in the absence of palmitic acid, *lip2* and, to a lesser extent, WT *C. albicans* triggered enhanced production of both IL-1β and IL-6 by BMDCs; however, both responses were blocked in the presence of 0.1 μM of palmitic acid (Figure 6B). As shown in Figure S5C, palmitic acid also suppresses BMDC activation (enhanced expression of IL-23) by strains expressing catalytically inactive alleles of *LIP2*. Note that fungal morphogenesis in the coculture assays (Figure S5D) and expression of *LIP2* by WT *C. albicans* (Figure S5E) are unaffected by palmitate. Finally, we confirmed that strains expressing WT *LIP2*, but not a *lip2* null mutant or strains expressing catalytically inactive *LIP2* point mutants, are able to hydrolyze a pNp-palmitate substrate (Figure 6C). Together, these results indicate that Lip2 liberates palmitic acid from suitable substrates and that palmitic acid suppresses BMDC activation by *C. albicans*.

The immune dampening effect of palmitic acid on DC activation by *C. albicans* was somewhat surprising in light of published reports that palmitic acid enhances the pro-inflammatory responses of macrophages and DCs to other pathogen-associated molecular patterns (PAMPs), thereby contributing to the morbidity of chronic diseases, such as obesity and type 2 diabetes mellitus, that are associated with elevated serum palmitate (Korbecki and Bajdak-Rusinek, 2019). In particular, one study reported that palmitic acid enhances BMDC activation (IL-23A production) in response to TLR agonists, including Pam3CSK4 (TLR1/TLR2 agonist), poly(I:C) (TLR3 homodimer agonist), LPS (TLR4 homodimer agonist), and imiquimod (TLR7/TLR8 agonist) (Mogilenko et al., 2019). We hypothesized that the distinct effect of palmitic acid on BMDCs in response to *C. albicans* reflects either a difference in our experimental assay or a difference in BMDC responses to live *lip2* yeasts compared with specific TLR agonists. To distinguish between these possibilities, we repeated our coculture experiments using both sets of assay conditions and included the published panel of TLR agonists as controls. Under our assay conditions, imiquimod was the only one of four tested TLR agonists to induce significant IL-23A production by BMDCs, and this response was substantially enhanced in the presence of 0.1 μM palmitic acid (Figure 6D). By comparison, coincubation with *lip2* yeasts triggered an even larger IL-23A response, and this response was suppressed by 0.1 μM palmitic acid (Figure 6D). Under the previously published assay conditions, which notably include a 24-h incubation period (compared with 2 h in our assay), LPS and imiquimod triggered significant IL-23A responses, and both responses were significantly enhanced in the presence of 500 μM palmitic acid (Figure S5F), as previously reported (Mogilenko et al., 2019). Coincubation with *lip2* also triggered IL-23A production under these assay conditions, and the response was suppressed by 500 μM palmitic acid (Figure S5F). These results confirm that BMDC activation by *lip2* occurs under both sets of assay conditions and suggest that the immune modulatory activity of palmitic acid can vary with the nature of the immune stimulus (pro-inflammatory with purified TLR agonists versus anti-inflammatory with whole yeast).

TLR2, TLR4, and Dectin-1 are cell-surface-associated pattern recognition receptors that have previously been implicated in host immune recognition of *C. albicans* (Netea et al., 2008). TLR2 and TLR4 are thought to recognize O-linked mannose residues, while Dectin-1 recognizes β-1,3-linked glycan residues of the fungal cell wall. To determine whether any of these receptors plays a role in the IL-23 response to *lip2*, we performed coculture assays with *C. albicans* and BMDCs prepared from *clec7a*$^{-/-}$ (Dectin-1 deficient), *tlr2*$^{-/-}$, *tlr4*$^{-/-}$, or *tlr2/tlr4*$^{-/-}$ mice. As shown in Figure 6E, *Clec7a* was found to be dispensable for BMDC activation by *lip2*, but the IL-23 response was significantly diminished in cells lacking *Tlr2* or *Tlr4* and virtually eliminated in cells lacking both *Tlr2* and *Tlr4*. These results suggest that TLR2 and TLR4 play nonredundant roles in BMDC activation by *C. albicans*.

(B) Palmitic acid also suppresses the IL1β and IL-6 responses of BMDCs to *lip2*. BMDCs from C57BL/6J mice were incubated with 0.1 μM palmitic acid or solvent alone, with or without WT *C. albicans* or *lip2* at an MOI of 1 for 2 h, followed by measurement of IL-1β or IL-6 in culture supernatants by ELISA. Statistical significance between the different conditions was determined by one-way ANOVA (Tukey's multiple comparisons test); ns: $p > 0.05$, *$p = 0.05$,***$p < 0.001$.

(C) Lip2 hydrolyzes pNp-palmitate to palmitic acid. WT *C. albicans*, *lip2*, *lip2+LIP2*, and strains expressing catalytically inactive Lip2 point mutants were propagated in BMDC culture medium to $OD_{600} = 1$, supernatants were incubated with pNp-palmitate, and hydrolysis was assessed by spectrophotometry. Statistical significance between the different mutants was determined by one-way ANOVA (Tukey's multiple comparisons test); **$p < 0.01$, ***$p < 0.001$, ****$p < 0.0001$.

(D) Palmitic acid dampens the BMDC response to *lip2* but enhances the response to imiquimod. BMDCs from C57BL/6J mice were incubated for 2 h with solvent (dark bars) or 0.1 μM palmitic acid (white bars), with or without TLR ligands (Pam3CSK4: TLR1/2; poly(I:C): TLR3; LPS: TLR4; imiquimod: TLR7/8) or *C. albicans* (WT or *lip2* at a MOI of 1), followed by measurement of IL-23A in cell supernatants by ELISA. Statistical significance between the solvent control and the PA conditions was determined by an unpaired two-tailed t test; ns: $p > 0.05$, **$p < 0.001$, ****$p < 0.0001$.

(E) TLR2 and TLR4 are required for BMDC activation by *C. albicans*. BMDCs from C57BL/6J mice were incubated with 0.1 μM fatty acids (palmitic acid, stearic acid, or linoleic acid) or solvent alone, with or without WT *C. albicans* or *lip2* at an MOI of 1 for 2 h, followed by measurement of IL-23A in cell supernatants by ELISA. Statistical significance between the different DCs infected with *lip2* was determined by one-way ANOVA (Tukey's multiple comparisons test); ns: $p > 0.05$, ****$p < 0.0001$.

DISCUSSION

Candida albicans is the primary fungus of the human gut microbiota and is among only a handful of fungal species to colonize humans. The perpetual association of *C. albicans* with mammalian hosts, paired with the absence of a known environmental reservoir, implies the existence of extensive coevolution between host and fungus. Indeed, it can be argued that *C. albicans* and humans enjoy a largely mutualistic relationship, with the fungus benefiting from a nutrient-rich, stable environment, and the host receiving certain immune benefits. Latter benefits include the stimulation of Th17-based immunity to other fungal pathogens, as well as a poorly understood, generalized resilience to fungi, bacteria, and viruses in diverse niches (Bacher et al., 2019; Jiang et al., 2017; Shao et al., 2019). Nevertheless, *C. albicans* remains a perpetual threat, with the ability to cause serious disease, particularly in hosts with risk factors for systemic infection.

Our screen of DOX-repressible GRACE mutants identified Lip2 as a fungal effector that is required for competitive fitness in kidneys (Figure 1A) and overall lethality (Figure 1B) in a murine model of systemic infection. Unlike most *C. albicans* mutants with defects in this model, a *lip2* null mutant is competent for yeast-to-hypha morphogenesis, both under laboratory conditions (Figures S1A and S1B) and in the host (Figures 1D and S1B). Further, after 1 h of infection, equal titers of *lip2* and WT can be recovered from kidneys, livers, and spleens, suggesting that the mutant is proficient in egress from the vasculature and penetration into target organs (Figures 1C and S2A). Instead, the first detectable deviation from standard bloodstream infections occurs at 6 h, when unusually high levels of pro-inflammatory cytokines (IL-23 and IL-17; Figures 2A, 2B, 4A, and S3A) are seen in *lip2*-infected kidneys. At subsequent time points, *lip2* displays progressive defects in persistence (Figures 1C and S2B–S2D) and damage to (Figures 1E and S2D) target organs, leading to the eradication of the infection (Figure 1C) and host survival (Figure 1B) in most cases.

Prior to this study, there were several reports of enhanced susceptibility to bloodstream candidiasis among mice with defects in IL-17 signaling (Huang et al., 2004; Ramani et al., 2018; Saijo et al., 2010). IL-17 was proposed to protect the host by increasing the resilience of kidneys during infection. Specifically, IL-17 was shown to activate the renal protective Kallikrein-Kinin proteolytic cascade and to exert direct anti-apoptotic activity on renal tubular epithelial cells (Ramani et al., 2016, 2018). Our finding that *lip2* is virulent in *Il17af*$^{-/-}$ animals but highly attenuated in WT littermates (Figures 3A–3E) suggests that IL-17 plays an additional role in the elimination of fungal pathogens from systemically infected animals. Medzhitov, Schneider, and Soares have hypothesized that injury from infectious disease is the result of pathogen proliferation plus host intolerance of the pathogen (Medzhitov et al., 2012). Viewed through this lens, our findings complement the published findings on renal tolerance (Ramani et al., 2016; Ramani et al., 2018) and suggest that IL-17 antagonizes both pathways of infection-related injury.

Following our identification of renal DCs as a source of IL-23A (Figure 4B) and renal TCR$\gamma\delta$+ T cells as a source of IL-17A (Figures 3F, 3G, and S3C) in *lip2*-infected kidneys, we tested whether *lip2* directly activates BMDCs in coculture experiments. The finding that IL-23A production is stimulated by strains lacking *LIP2* (Figure 4D) or expressing catalytically inactive *LIP2* point mutants (Figure 5C), but not WT *C. albicans*, suggested that a Lip2-dependent metabolite might suppress the activation of BMDCs. Consistent with this model, exposure of cocultured cells to 0.1 μM palmitic acid suppresses induction of IL-23A (as well as IL-1β and IL-6; Figures 6A and 6B). Interestingly, the immune dampening effect of palmitic acid on BMDCs in response to a fungal stimulus is opposite to its published pro-inflammatory effects in response to multiple TLR agonists (Mogilenko et al., 2019). Although we have yet to define which features of the *lip2* mutant (or HK WT cells, Figure 4F) are sensed by DCs, TLR2 and TLR4 appear to be required for the full response (Figure 6E).

In sum, our results support a model in which Lip2 promotes fungal virulence by suppressing the host IL-17 response. We propose that, in organs such as the kidney, Lip2 increases the local concentration of immune modulatory fatty acids such as palmitic acid, thereby blunting TLR2- and TLR4-dependent activation of tissue-resident DCs. The immune dampening effect may be mediated directly on DCs or may be indirect, for example, because of decreased expression of TLR2/TLR4 ligands on the *C. albicans* cell surface. In contrast, during infections with *C. albicans* mutants that lack *LIP2* or express catalytically inactive versions of the enzyme, DCs are activated to release IL-23, leading to IL-17 expression by tissue-resident TCR$\gamma\delta$+ T cells. The lipid-mediated suppression of IL-17 that we observe in solid organs is apparently not active in skin (Kashem et al., 2015), where IL-17 is known to play an active role in suppressing the proliferation of *C. albicans*. This difference may be related to the observation that, in skin, *C. albicans* is sensed by nociceptive sensory fibers, which leads to DC activation and IL-17 production by dermal TCR$\gamma\delta$+ T cells (Kashem et al., 2015). This neuro-immune pathway may bypass the Lip2-mediated DC suppression that we observe in solid organs. Future work will be needed to clarify whether Lip2 plays a role in mucocutaneous candidiasis.

STAR★METHODS

Detailed methods are provided in the online version of this paper and include the following:

- KEY RESOURCES TABLE
- RESOURCE AVAILABILITY
  - Lead contact
  - Materials availability
  - Data and code availability
- EXPERIMENTAL MODEL AND SUBJECT DETAILS
  - Yeast manipulations
  - Studies in animals
- METHOD DETAILS
  - Determination of competitive index
  - Histology
  - Kidney dissociation and recovery of renal dendritic cells
  - Flow cytometry

- RNA isolation and RT-qPCR
- Preparation of BMDCs
- In vitro activation of dendritic cells
- Measurement of cytokine production
- Lipase activity assay
- pNp-Palmitate Hydrolase Activity Assay
- Immunoblotting

● QUANTIFICATION AND STATISTICAL ANALYSIS

SUPPLEMENTAL INFORMATION

Supplemental information can be found online at https://doi.org/10.1016/j.chom.2022.10.004.

ACKNOWLEDGMENTS

We are grateful to Prof. Gregory Barton (UC Berkeley) for the gift of *tlr2*$^{-/-}$, *tlr4*$^{-/-}$, and *tlr2,4*$^{-/-}$ femurs, and to Prof. Richard Locksley (UCSF) for the gift of SMART17 mice. We thank Allison Cohen for technical advice on the preparation of BMDCs. Finally, we are indebted to Prof. Anita Sil (UCSF), Prof. Sarah L. Gaffen (U. Pittsburg), and Prof. Partha S. Biswas (U. Pittsburg) for illuminating discussions and advice. We thank Merck and Genome Canada for making the original *C. albicans* GRACE mutant collections available. This work was funded by R01AI127375 to S.M.N. and L.E.C., and R01AI00272 and R01 AI165541 to H.D.M. E.V.D. was supported by a Damon Runyon Postdoctoral Fellowship. L.E.C. is a Canada Research Chair (Tier 1) in Microbial Genomics & Infectious Disease and co-director of the CIFAR Fungal Kingdom: Threats & Opportunities program. L.E.C. is a co-founder and shareholder in Bright Angel Therapeutics, a platform company for the development of novel antifungal therapeutics.

AUTHOR CONTRIBUTIONS

Conceptualization, P.B. and S.M.N.; methodology, P.B., E.V.D., and S.M.N.; investigation, P.B. and E.V.D.; visualization, P.B., A.U., and S.M.N.; funding acquisition, H.D.M., L.E.C., and S.M.N.; project administration, S.M.N.; supervision, H.D.M., L.E.C., and S.M.N.; writing – original draft, P.B. and S.M.N.; writing – review & editing, P.B., E.V.D., H.D.M., and S.M.N.

DECLARATION OF INTERESTS

The authors declare no competing interests.

Received: February 16, 2022
Revised: August 17, 2022
Accepted: October 5, 2022
Published: November 1, 2022

REFERENCES

Bacher, P., Hohnstein, T., Beerbaum, E., Röcker, M., Blango, M.G., Kaufmann, S., Röhmel, J., Eschenhagen, P., Grehn, C., Seidel, K., et al. (2019). Human anti-fungal Th17 immunity and pathology rely on cross-reactivity against *Candida albicans*. Cell *176*. 1340–1355.e15. https://doi.org/10.1016/j.cell.2019.01.041.

Bonventre, J.V. (2014). Kidney injury molecule-1: a translational journey. Trans. Am. Clin. Climatol. Assoc. *125*, 293–299 discussion 299.

Brown, G.D., Denning, D.W., Gow, N.A., Levitz, S.M., Netea, M.G., and White, T.C. (2012). Hidden killers: human fungal infections. Sci. Transl. Med. *4*, 165rv113. https://doi.org/10.1126/scitranslmed.3004404.

Conti, H.R., Shen, F., Nayyar, N., Stocum, E., Sun, J.N., Lindemann, M.J., Ho, A.W., Hai, J.H., Yu, J.J., Jung, J.W., et al. (2009). Th17 cells and IL-17 receptor signaling are essential for mucosal host defense against oral candidiasis. J. Exp. Med. *206*, 299–311. https://doi.org/10.1084/jem.20081463.

Denning, D.W., Kneale, M., Sobel, J.D., and Rautemaa-Richardson, R. (2018). Global burden of recurrent vulvovaginal candidiasis: a systematic review. Lancet Infect. Dis. *18*, e339–e347. https://doi.org/10.1016/S1473-3099(18)30103-8.

Edmond, M.B., Wallace, S.E., McClish, D.K., Pfaller, M.A., Jones, R.N., and Wenzel, R.P. (1999). Nosocomial bloodstream infections in United States hospitals: a three-year analysis. Clin. Infect. Dis. *29*, 239–244.

Hallen-Adams, H.E., and Suh, M.J. (2017). Fungi in the healthy human gastrointestinal tract. Virulence *8*, 352–358. https://doi.org/10.1080/21505594.2016.1247140.

Huang, W., Na, L., Fidel, P.L., and Schwarzenberger, P. (2004). Requirement of interleukin-17A for systemic anti-*Candida albicans* host defense in mice. J. Infect. Dis. *190*, 624–631. https://doi.org/10.1086/422329.

Hube, B., Steh, F., Bossenz, M., Mazur, A., Kretschmar, M., and Schäfer, W. (2000). Secreted lipases of *Candida albicans*: cloning, haracterisation and expression analysis of a new gene family with at least ten members. Arch. Microbiol. *174*, 362–374. https://doi.org/10.1007/s002030000218.

Huppler, A.R., Bishu, S., and Gaffen, S.L. (2012). Mucocutaneous candidiasis: the IL-17 pathway and implications for targeted immunotherapy. Arthritis Res. Ther. *14*, 217. https://doi.org/10.1186/ar3893.

Jackson, B.E., Wilhelmus, K.R., and Hube, B. (2007). The role of secreted aspartyl proteinases in *Candida albicans* keratitis. Invest. Ophthalmol. Vis. Sci. *48*, 3559–3565. https://doi.org/10.1167/iovs.07-0114.

Jiang, T.T., Shao, T.Y., Ang, W.X.G., Kinder, J.M., Turner, L.H., Pham, G., Whitt, J., Alenghat, T., and Way, S.S. (2017). Commensal fungi recapitulate the protective benefits of intestinal bacteria. Cell Host Microbe *22*. 809–816.e4. https://doi.org/10.1016/j.chom.2017.10.013.

Kashem, S.W., Riedl, M.S., Yao, C., Honda, C.N., Vulchanova, L., and Kaplan, D.H. (2015). Nociceptive sensory fibers drive interleukin-23 production from CD301b+ dermal dendritic cells and drive protective cutaneous immunity. Immunity *43*, 515–526. https://doi.org/10.1016/j.immuni.2015.08.016.

Korbecki, J., and Bajdak-Rusinek, K. (2019). The effect of palmitic acid on inflammatory response in macrophages: an overview of molecular mechanisms. Inflamm. Res. *68*, 915–932. https://doi.org/10.1007/s00011-019-01273-5.

Lévy, R., Okada, S., Béziat, V., Moriya, K., Liu, C., Chai, L.Y.A., Migaud, M., Hauck, F., Al Ali, A., Cyrus, C., et al. (2016). Genetic, immunological, and clinical features of patients with bacterial and fungal infections due to inherited IL-17RA deficiency. Proc. Natl. Acad. Sci. USA *113*, E8277–E8285. https://doi.org/10.1073/pnas.1618300114.

Ling, Y., Cypowyj, S., Aytekin, C., Galicchio, M., Camcioglu, Y., Nepesov, S., Ikinciogullari, A., Dogu, F., Belkadi, A., Levy, R., et al. (2015). Inherited IL-17RC deficiency in patients with chronic mucocutaneous candidiasis. J. Exp. Med. *212*, 619–631. https://doi.org/10.1084/jem.20141065.

Lionakis, M.S., Lim, J.K., Lee, C.C., and Murphy, P.M. (2011). Organ-specific innate immune responses in a mouse model of invasive candidiasis. J. Innate Immun. *3*, 180–199. https://doi.org/10.1159/000321157.

Livak, K.J., and Schmittgen, T.D. (2001). Analysis of relative gene expression data using real-time quantitative PCR and the $2^{-\Delta\Delta C}_{T}$ method. Methods *25*, 402–408. https://doi.org/10.1006/meth.2001.1262.

Medzhitov, R., Schneider, D.S., and Soares, M.P. (2012). Disease tolerance as a defense strategy. Science *335*, 936–941. https://doi.org/10.1126/science.1214935.

Mogilenko, D.A., Haas, J.T., L'Homme, L., Fleury, S., Quemener, S., Levavasseur, M., Becquart, C., Wartelle, J., Bogomolova, A., Pineau, L., et al. (2019). Metabolic and innate immune cues merge into a specific inflammatory response via the UPR. Cell *178*, 263. https://doi.org/10.1016/j.cell.2019.06.017.

Moyes, D.L., Wilson, D., Richardson, J.P., Mogavero, S., Tang, S.X., Wernecke, J., Höfs, S., Gratacap, R.L., Robbins, J., Runglall, M., et al. (2016). Candidalysin is a fungal peptide toxin critical for mucosal infection. Nature *532*, 64–68. https://doi.org/10.1038/nature17625.

Netea, M.G., Brown, G.D., Kullberg, B.J., and Gow, N.A. (2008). An integrated model of the recognition of *Candida albicans* by the innate immune system. Nat. Rev. Microbiol. *6*, 67–78.

Noble, S.M., French, S., Kohn, L.A., Chen, V., and Johnson, A.D. (2010). Systematic screens of a *Candida albicans* homozygous deletion library

decouple morphogenetic switching and pathogenicity. Nat. Genet. *42*, 590–598. https://doi.org/10.1038/ng.605.

Noble, S.M., Gianetti, B.A., and Witchley, J.N. (2017). *Candida albicans* cell-type switching and functional plasticity in the mammalian host. Nat. Rev. Microbiol. *15*, 96–108. https://doi.org/10.1038/nrmicro.2016.157.

Noble, S.M., and Johnson, A.D. (2005). Strains and strategies for large-scale gene deletion studies of the diploid human fungal pathogen *Candida albicans*. Eukaryot. Cell *4*, 298–309.

O'Meara, T.R., Veri, A.O., Ketela, T., Jiang, B., Roemer, T., and Cowen, L.E. (2015). Global analysis of fungal morphology exposes mechanisms of host cell escape. Nat. Commun. *6*, 6741. https://doi.org/10.1038/ncomms7741.

Pfaller, M., Neofytos, D., Diekema, D., Azie, N., Meier-Kriesche, H.U., Quan, S.P., and Horn, D. (2012). Epidemiology and outcomes of candidemia in 3648 patients: data from the prospective antifungal therapy (PATH Alliance®) registry, 2004–2008. Diagn. Microbiol. Infect. Dis. *74*, 323–331. https://doi.org/10.1016/j.diagmicrobio.2012.10.003.

Pfaller, M.A., and Diekema, D.J. (2007). Epidemiology of invasive candidiasis: a persistent public health problem. Clin. Microbiol. Rev. *20*, 133–163. https://doi.org/10.1128/CMR.00029-06.

Pfaller, M.A., Pappas, P.G., and Wingard, J.R. (2006). Invasive fungal pathogens: current epidemiological trends. Clin. Infect. Dis. *43*, S3–S14.

Price, A.E., Reinhardt, R.L., Liang, H.E., and Locksley, R.M. (2012). Marking and quantifying IL-17A-producing cells in vivo. PLoS One *7*, e39750. https://doi.org/10.1371/journal.pone.0039750.

Puel, A., Cypowyj, S., Bustamante, J., Wright, J.F., Liu, L., Lim, H.K., Migaud, M., Israel, L., Chrabieh, M., Audry, M., et al. (2011). Chronic mucocutaneous candidiasis in humans with inborn errors of interleukin-17 immunity. Science *332*, 65–68. https://doi.org/10.1126/science.1200439.

Rajendran, R., Lew, S.K., Yong, C.X., Tan, J., Wang, D.J., and Chuang, K.H. (2013). Quantitative mouse renal perfusion using arterial spin labeling. NMR Biomed. *26*, 1225–1232. https://doi.org/10.1002/nbm.2939.

Ramani, K., Garg, A.V., Jawale, C.V., Conti, H.R., Whibley, N., Jackson, E.K., Shiva, S.S., Horne, W., Kolls, J.K., Gaffen, S.L., and Biswas, P.S. (2016). The kallikrein-kinin system: a novel mediator of IL-17-driven anti-candida immunity in the kidney. PLoS Pathog. *12*, e1005952. https://doi.org/10.1371/journal.ppat.1005952.

Ramani, K., Jawale, C.V., Verma, A.H., Coleman, B.M., Kolls, J.K., and Biswas, P.S. (2018). Unexpected kidney-restricted role for IL-17 receptor signaling in defense against systemic *Candida albicans* infection. JCI Insight *3*, e98241. https://doi.org/10.1172/jci.insight.98241.

Roemer, T., Jiang, B., Davison, J., Ketela, T., Veillette, K., Breton, A., Tandia, F., Linteau, A., Sillaots, S., Marta, C., et al. (2003). Large-scale essential gene identification in *Candida albicans* and applications to antifungal drug discovery. Mol. Microbiol. *50*, 167–181.

Saijo, S., Ikeda, S., Yamabe, K., Kakuta, S., Ishigame, H., Akitsu, A., Fujikado, N., Kusaka, T., Kubo, S., Chung, S.H., et al. (2010). Dectin-2 recognition of alpha-mannans and induction of Th17 cell differentiation is essential for host defense against *Candida albicans*. Immunity *32*, 681–691. https://doi.org/10.1016/j.immuni.2010.05.001.

Shao, T.Y., Ang, W.X.G., Jiang, T.T., Huang, F.S., Andersen, H., Kinder, J.M., Pham, G., Burg, A.R., Ruff, B., Gonzalez, T., et al. (2019). Commensal *Candida albicans* positively calibrates systemic Th17 immunological responses. Cell Host Microbe *25*. 404–417.e6. https://doi.org/10.1016/j.chom.2019.02.004.

Sparber, F., and Leibundgut-Landmann, S. (2019). Interleukin-17 in antifungal immunity. Pathogens *8*, 54. https://doi.org/10.3390/pathogens8020054.

Stoldt, V.R., Sonneborn, A., Leuker, C.E., and Ernst, J.F. (1997). Efg1p, an essential regulator of morphogenesis of the human pathogen *Candida albicans*, is a member of a conserved class of bHLH proteins regulating morphogenetic processes in fungi. EMBO J. *16*, 1982–1991. https://doi.org/10.1093/emboj/16.8.1982.

Sutton, C.E., Lalor, S.J., Sweeney, C.M., Brereton, C.F., Lavelle, E.C., and Mills, K.H. (2009). Interleukin-1 and IL-23 induce innate IL-17 production from gammadelta T cells, amplifying Th17 responses and autoimmunity. Immunity *31*, 331–341. https://doi.org/10.1016/j.immuni.2009.08.001.

STAR★METHODS

KEY RESOURCES TABLE

REAGENT or RESOURCE	SOURCE	IDENTIFIER
Antibodies		
Brilliant Violet 785 anti-mouse CD11b (M1/70)	Biolegend	Cat# 101243; RRID: AB_2561373
PE-Cy7 anti-mouse CD11c (N418)	Biolegend	Cat# 117317; RRID: AB_493569
Pacific Blue anti-mouse CD45.2 (104)	Biolegend	Cat# 109819; RRID: AB_492873
Brilliant Violet 785 anti-mouse CD90.2 (30-H12)	Biolegend	Cat# 105331; RRID: AB_893442
Brilliant Violet 605 anti-mouse CD45R/B220 (RA3-6B2)	Biolegend	Cat# 103243; RRID: AB_11203907
PE anti-mouse IL-17A (TC11-18H10.1)	Biolegend	Cat# 506903; RRID: AB_315463
PerCP/Cyanine5.5 anti-mouse TCR gamma delta (GL3)	Biolegend	Cat# 118117; RRID:AB_10612572
PE anti-mouse MHCII (I-A/I-E) (M5/114.15.2)	Biolegend	Cat# 100348; RRID:AB_2564029
FITC anti-mouse CD4 (GK1.5)	Biolegend	Cat# 100405; RRID: AB_312690
Brilliant Violet 785 anti-mouse CD11b (M1/70)	Biolegend	Cat# 101243; RRID: AB_2561373
PE-Cy7 anti-mouse CD11c (N418)	Biolegend	Cat# 117317; RRID: AB_493569
Pacific Blue anti-mouse CD45.2 (104)	Biolegend	Cat# 109819; RRID: AB_492873
anti-FLAG	Thermo Fisher Scientific	Cat# MA1-142-A488; RRID:AB_2610653
Chemicals, peptides, and recombinant proteins		
Acid phenol chloroform	Ambion	AM9722
Phenol chloroform isoamyl alcohol	Ambion	AM9732
Recombinant mouse GM-CSF	Prepotech	Cat# 315-03
IL-4	Gibco	Cat# PMC0045
Pam3CSK4	InvivoGen	Cat# tlrl-pms
Poly(I:C)	InvivoGen	Cat# tlrl-pic
LPS from E.coli	Sigma	Cat# L3024
Imiquimod	Calbiochem	Cat# CAS 99001-02-6
Palmitic acid	Sigma	Cat# P0500
Stearic acid	Sigma	Cat# S4751
Linoleic acid	Sigma	Cat #L1376
RPMI media	UCSF Media Production	Cat# CCFAE001
FBS	UCSF Media Production	Cat# CCFAQ009
Bovine serum Albumin	Sigma	Cat# A6003
Percoll	Cytivia	Cat# 17089101
PMA	Sigma	Cat# P1585
Ionomycin	Sigma	Cat# I9657
GolgiStop	Fisher Scientific	Cat# BDB555029
BD Cytofix buffer	Fisher Scientific	Cat# BDB554655
Perm/Wash reagent	BD Biosciences	Cat# BDB554723
Critical commercial assays		
Collagenase I	Thermo Fisher Scientific	Cat# 17100017
DNAse I	Thermo Fisher Scientific	Cat# EN0521
RNeasy Plus mini kit	Qiagen	Cat# 74134
DuoSet ELISA kit IL-23	R&D Systems	Cat# DY1887

(*Continued on next page*)

Continued

REAGENT or RESOURCE	SOURCE	IDENTIFIER
DuoSet ELISA kit IL-17	R&D Systems	Cat# DY421
DuoSet ELISA kit IL-1	R&D Systems	Cat# DY401
DuoSet ELISA kit IL-6	R&D Systems	Cat# DY406
Lipase Assay Kit	Sigma	Cat# MAK046
pNp-palmitate	Sigma	Cat# N2752
Trizol reagent	ThermoFisher	Cat# 15596026
SYBR Green Master Mix	Biorad	Cat# 1725275
Superscript III	Invitrogen	Cat# 18080
Experimental models: Cell lines		
Bone marrow-derived dendritic cells differentiated in the presence of GM-CSF and IL-4	This paper	N/A
Experimental models: Organisms/strains		
Mouse: BALB/c	Charles River Laboratories	Stock No: 028
Mouse: C57BL/6J	Jackson Laboratories	Stock no. 000664
Mouse: il17af$^{-/-}$	Jackson Laboratories	Stock no. 034140
SN2019	This study	WT control strain for *lip2*$^{DOX-OFF}$
SN2464	Roemer et al., 2003	*lip2*$^{DOX-OFF}$
SN250	Noble et al., 2010	*leu2Δ::C.d.LEU2/leu2Δ::C.m.HIS1*, *his1Δ/his1Δ*, *arg4Δ/arg4Δ*, *ura3Δ/URA3*, *iro1/IRO1*
SN2461	Noble et al., 2010	*lip2Δ::C.d.LEU2/lip2Δ::C.m.HIS1*, *his1Δ/his1Δ*, *arg4Δ/arg4Δ*, *ura3Δ/URA3*, *iro1/IRO1*
SN2242	This study	*LIP2/lip2Δ*, *leu2Δ::C.d.LEU2/leu2Δ::C.m.HIS1*, *his1Δ/his1Δ*, *arg4Δ::C.d.ARG4/arg4Δ*, *ura3Δ/URA3*, *iro1/IRO1*
SN2243	This study	*LIP2*^{S196A}*/lip2Δ*, *leu2Δ::C.d.LEU2/leu2Δ::C.m.HIS1*, *his1Δ/his1Δ*, *arg4Δ::C.d.ARG4/arg4Δ*, *ura3Δ/URA3*, *iro1/IRO1*
SN2246	This study	*LIP2*^{D240A}*/lip2Δ*, *leu2Δ::C.d.LEU2/leu2Δ::C.m.HIS1*, *his1Δ/his1Δ*, *arg4Δ::C.d.ARG4/arg4Δ*, *ura3Δ/URA3*, *iro1/IRO1*
SN2250	This study	*LIP2*^{H344A}*/lip2Δ*, *leu2Δ::C.d.LEU2/leu2Δ::C.m.HIS1*, *his1Δ/his1Δ*, *arg4Δ::C.d.ARG4/arg4Δ*, *ura3Δ/URA3*, *iro1/IRO1*
SN2253	This study	*LIP2*^{S196A,D240A,H344A}*/lip2Δ*, *leu2Δ::C.d.LEU2/leu2Δ::C.m.HIS1*, *his1Δ/his1Δ*, *arg4Δ::C.d.ARG4/arg4Δ*, *ura3Δ/URA3*, *iro1/IRO1*
SN119	Noble and Johnson, 2005	*efg1Δ::C.d.HIS1/efg1Δ::C.m.LEU2*, *leu2Δ/leu2Δ*, *his1Δ/his1Δ*, *ura3Δ/URA3*, *iro1/IRO1*
SN2462	Noble et al., 2010	*ece1Δ::C.d.LEU2/ece1Δ::C.m.HIS*, *leu2Δ/leu2Δ*, *his1Δ/his1Δ*, *arg4Δ/arg4Δ*, *ura3Δ/URA3*, *iro1/IRO1*
SN1664	Noble et al., 2010	*sap6Δ::C.d.LEU2/sap6Δ::C.m.HIS*, *leu2Δ/leu2Δ*, *his1Δ/his1Δ*, *arg4Δ/arg4Δ*, *ura3Δ/URA3*, *iro1/IRO1*

(*Continued on next page*)

Continued		
REAGENT or RESOURCE	SOURCE	IDENTIFIER
SN2463	Noble et al., 2010	*lip10Δ::C.d.LEU2/lip10Δ::C.m.HIS*, *leu2Δ/leu2Δ*, *his1Δ/his1Δ*, *arg4Δ/arg4Δ*, *ura3Δ/URA3*, *iro1/IRO1*
Oligonucleotides		
Oligonucleotides are described in Table S1	N/A	N/A

RESOURCE AVAILABILITY

Lead contact

Further information and requests for reagents may be directed to and will be fulfilled by the Lead Contact, Suzanne M. Noble (suzanne.noble@ucsf.edu).

Materials availability

C. albicans strains in this study will be made available on request, but may require payment and/or a completed Materials Transfer Agreement if there is potential for commercial application.

Data and code availability

- All data reported in this paper will be shared by the lead contact upon request.
- This paper does not report original code.
- Any additional information required to reanalyze the data reported in this work is available from the Lead Contact upon request.

EXPERIMENTAL MODEL AND SUBJECT DETAILS

Yeast manipulations

Yeast strains and primers used for this study are described in key resources table, and Table S1. Growth assays were performed with strains that were freshly streaked from frozen glycerol stocks onto YPD agar and incubated for two days at 30°C. A single colony was suspended in sterile distilled water to an optical density at 600 nm (OD_{600}) of 1 and diluted as appropriate for the assay. New strains were constructed as described in (Noble and Johnson, 2005).

Studies in animals

All procedures involving animals were approved by the Institutional Animal Care and Use Committee at the University of California San Francisco and were carried out according to the National Institute of Health (NIH) guidelines for the ethical treatment of animals. Experiments were performed with 8–10 week female BALB/c (no.028) mice from Charles River Laboratories or eight-week-old (male and female) C57BL/6J (no. 000664) WT and il17af$^{-/-}$ (no. 034140) mice from Jackson Laboratories and bred in-house. Systemic infection was performed by inoculation of 1×10^5 CFUs (BALB/C), 1×10^6 CFUs (WT C57BL/6J) or 5×10^5 CFUs (il17af$^{-/-}$ C57BL/6J) of mid-log phase yeasts into the retro bulbar sinus of animals, under isoflurane anesthesia. Animals were monitored closely and euthanized at the experimentally determined endpoints or upon development of signs of clinical morbidity (defined as BCS $\leq$ 2, hunched posture, decreased motor activity), whichever was first. Kidneys were then recovered for CFU analysis, histology, RNA analysis, and/or analysis of competitive fitness. Female BALB/C infected with the *lip2*(DOX-OFF) strain were additionally treated with 0.25 mg/mL of doxycycline via drinking water beginning seven days prior to infection and continued throughout the experiment.

METHOD DETAILS

Determination of competitive index

Competitive index (CI) of strains in 1:1 competitive infections of the systemic infection model was determined as in (Noble et al., 2010). Strain abundance was determined by qPCR of genomic DNA prepared from colonies plated on Sabouraud agar recovered from the inoculum and infected kidneys, using strain-specific primers (Table S1) and a Roche LightCycler 480 instrument. The significance of observed differences was determined using the paired Student's t-test.

Histology

Kidneys were fixed in 10% formalin for 24 hours and washed in 80% ethanol. Preparation of paraffin blocks and 4 μm sections as well as staining with PAS and H&E were performed by Nationwide Histology (MT).

Kidney dissociation and recovery of renal dendritic cells

Kidneys were minced and digested with Collagenase I (0.125mg/mL, Thermo Fisher Scientific), DNAse I (0.2 mg/mL, Millipore) in RPMI with 10% of FBS for 30 min at 37°C, prior to filtration through a 100-micron strainer (Thermo Fisher Scientific) and washing with RPMI + 2% FBS + 5 mM EDTA. Cells were suspended in FACS buffer (PBS, 2% FBS, 1 mM EDTA) and purified over a discontinuous gradient of 70% and 30% Percoll (Cytivia). Cells collected from the 70%-30% interface were washed in FACS buffer for further analysis.

Isolation of renal DCs: Cells recovered from the Percoll gradient were suspended in MACS buffer and incubated with CD11c-Ab beads for 15 min at 4°C. CD11c+ DCs were isolated using MS MACS columns per the manufacturer's instructions. Quantitation was performed with a hemocytometer, and total RNA was extracted using an RNeasy Plus mini kit (Qiagen).

Flow cytometry

Cells were stained with antibodies against TCRgd (GL3), CD4 (GK1.5), B220 (RA3-6B2), CD45 (30-F11), IL-17A (TC11-18H10.1), hNGFR (ME20.4), CD90.2 (53-2.1), CD11b (M1/70) Ly6G (1A8), CD11c (N418), F4/80 (BM8), MHCII (M5/114.15.2) (from Biolegend, BD Biosciences or eBiosciences). To determine the source of IL-17A in kidneys, dissociated cells were incubated for two hours in MACS buffer supplemented with PMA (50 ng/ml) and ionomycin (500 ng/ml) with GolgiStop (1000X). To detect intracellular IL-17A, cells were treated with BD Cytofix buffer and Perm/Wash reagent (BD Biosciences) and then stained with anti-IL-17A (C57BL/6J) or anti-hNGFR (SMART17 C57BL/6J) in Perm/wash buffer. Samples were analyzed by FACS (BD), and data were analyzed with FlowJo software (Version 10, BD, https://www.flowjo.com/).

RNA isolation and RT-qPCR

Isolation of total RNA from kidneys or dendritic cells was performed using TriZol or RNeasy Plus Mini kits per the manufacturer's protocols. First-strand complementary DNA (cDNA) was synthesized from 1 μg of total RNA using the Superscript III cDNA Reverse Transcription Kit (Thermo Fisher Scientific). Quantitative PCR was performed with specific primers described in Table S1. We employed the ΔΔCt method (Livak and Schmittgen, 2001); results were normalized to the housekeeping genes *Gadph or ACT1* for *LIP2* and *LIP10* expression.

Preparation of BMDCs

Bone-marrow-derived dendritic cells (BMDC) were isolated from femurs and tibias of 6- to 8-week old (male and female) C57BL/6J mice (WT, *tlr2*$^{-/-}$, *tlr4*$^{-/-}$, *tlr2*$^{-/-}$*4*$^{-/-}$, *clec7a*$^{-/-}$). Bone marrow was eluted from bones with RPMI + 5% FBS and filtered through a cell strainer (70 μm). The cell suspension was centrifuged at 250 × g for 5 min at 4°C, and the pellet was re-suspended in 2 ml of RPMI + 5% FBS and 1 mL/mouse of ACK erythrocyte lysis buffer (Ammonium-Chloride-Potassium Lysing Buffer, Thermo Fisher Scientific). After incubation for 7 min one ice, 20 mL PBS was added before centrifugation, and pellets were washed once in RPMI. Cells were plated onto 100 mm non-tissue culture treated culture plate in complete RPMI (10% FCS, 10 μM 2-mercaptoethanol, 25 mM HEPES, Glutamax 100X, 100 U/mL penicillin, 100 μg/mL of streptomycin sulfate and 20 ng/mL GM-CSF (Prepotech)) for three days. On day three, cells were treated with ten mL of complete RPMI. On days six, eight, and ten, adherent cells were collected, washed, and plated with a Complete RPMI supplemented with 10 ng/mL of IL-4 (Gibco). Mature DCs were used on day 12.

In vitro activation of dendritic cells

Murine BMDCs were seeded into 24-well tissue culture-treated plates (BD) at 1x10^5 cells per well in one ml complete RPMI (without penicillin and streptomycin) and cultured O/N at 37°C in 5% CO_2. Activation by specific *C. albicans* strains was assessed after co-incubation for two hours at MOI 1, followed by measurement of IL-23 in cell supernatants by ELISA.

Free fatty acid (FFA) supplementation. FFA (in chloroform) was added to BMDCs in culture medium to a final concentration of 1, 0.1, 0.01 μM for two hours.

Activation of DCs by TLR ligands. 5x10^5 cells/mL were incubated in complete RPMI and treated with 100 ng/mL Pam3CSK4, 10 μg/mL Poly(I:C), 100 ng/mL LPS, or 3 μg/mL imiquimod with or without palmitic acid conjugated with BSA when mentioned. Cells were activated for 24 hours or 2 hours.

Measurement of cytokine production

Cytokine production was measured by enzyme-linked immunoassay using a DuoSet ELISA kit (R&D Systems) following the manufacturer's protocol. Briefly, for detection of IL-17A, and IL-23A, 200 μL of kidney homogenate was used. For *in vitro* coculture experiments with BMDCs, 100 μL of cell supernatant was used to detect IL-23A, IL1 β, and IL6.

Lipase activity assay

Lipase activity was assessed with a Lipase Assay Kit (Sigma). Briefly, strains were propagated in liquid YPD to an OD_{600} of 1. One mL of each culture was pelleted, and 100 μL of the supernatant was used for the assay.

pNp-Palmitate Hydrolase Activity Assay

Lipase activity was assayed spectrophotometrically using pNp-palmitate as a substrate. The reaction buffer was composed of 50 mM Tris-HCl pH 8, 1 mg/mL Arabic gum, 0.005% of Triton X-100, and 3.9 mM pNp-palmitate (Sigma). Strains were grown in

dendritic cell media to A_{600} of 1. 5 mL of supernatant was concentrated using concentrator tubes (Thermo Fisher Scientific) for a final volume of one ml. Samples were incubated at 30°C in the dark for 15 min, and absorbance was read at 410 nm.

Immunoblotting

Strains were propagated in liquid YPD at 30°C O/N. Supernatants from 10 mL of pelleted cultures were concentrated using protein concentrator tubes (Pierce), denatured in Laemmli buffer, and boiled at 100°C for 10 min. 15 μL of each sample was analyzed by SDS-PAGE and immunoblotted with anti-FLAG (Thermo Fisher Scientific).

QUANTIFICATION AND STATISTICAL ANALYSIS

Competitive fitness assays (competitive index of mutant versus WT in the systemic infection model) are presented with a single dot representing the CI of each *C. albicans* strain in each mouse (biological) replicate, based on the average of three technical replicates. A bar represents the median CI. Fungal burden in infected organs (CFU of *C. albicans*/gram organ) are presented as the mean of three independent biological replicates. RNA expression is presented as the mean of three biological replicates, each based on the average of three technical replicates. ELISA assays (cytokine protein levels) are presented as the mean of at least three biological replicates; in some figures the results of individual biological replicates are indicated as dots. Error bars depict the standard error of the mean (SEM)

Statistical analyses were performed using GraphPad Prism 9.2 (Graphpad Software). Statistical significance was analyzed by the Student's t-test (CFU analysis, mRNA expression, cytokine levels, competitive fitness), One-way ANOVA (with Tukey's correction for multiple comparisons; CFU analysis, mRNA expression, flow cytometry measurements), or the Mantel-Cox test (survival curve), as indicated in the figure legends. No methods were used to determine whether the data met assumptions of the statistical approaches. Significant differences are indicated as *p<0.05; **p <0.01; ***p<0.001; ****p<0.0001.